MARTIN MARIETTA ENERGY SYSTEMS LIBRARIES
3 4456 0352764 5

ORNL 1033
Progress Report
90

AEC RESEARCH AND DEVELOPMENT REPORT

METALLURGY DIVISION

QUARTERLY PROGRESS REPORT

for Period Ending April 30, 1951

LIBRARY
DO NOT TRANSFER
If you wish someone el... send in name with docu... arrange a loan.

OAK RIDGE NATIONAL LABORATORY
OPERATED BY
CARBIDE AND CARBON CHEMICALS COMPANY
A DIVISION OF UNION CARBIDE AND CARBON CORPORATION
POST OFFICE BOX P
OAK RIDGE, TENNESSEE

DECLASSIFIED
CLASSIFICATION CHANGED TO:
BY AUTHORITY OF: AEC 10-9-59
BY: 60

[redacted]

ORNL-1033
Progress Report

This document consists of 82 pages.
Copy 9 of 137. Series A.

Contract No. W-7405, eng 26

METALLURGY DIVISION

J. H. Frye, Jr. Director

QUARTERLY PROGRESS REPORT

for Period Ending April 30, 1951

Edited by:

E. C. Miller and W. H. Bridges

Date Issued OCT 1951

MARTIN MARIETTA ENERGY SYSTEMS LIBRARIES

3 4456 0352764 5

OAK RIDGE NATIONAL LABORATORY
operated by
CARBIDE AND CARBON CHEMICALS COMPANY
A Division of Union Carbide and Carbon Corporation
Post Office Box P
Oak Ridge, Tennessee

[redacted] as defined in the Atomic Energy Act of 1946.

[redacted] This [redacted] information affecting the Na[redacted] Its [redacted] a[redacted] prohibited [redacted] criminal penalties under applicable Federal laws.

[redacted]

ORNL-1033
Progress Report

INTERNAL

1. G. T. Felbeck (C&CCC)
2-3. Chemistry Library
4. Physics Library
5. Biology Library
6. Health Physics Library
7. Metallurgy Library
8-9 Training School Library
10-13 Central Files
14. C. E. Center
15. C. E. Larson
16 W. B. Humes (K-25)
17. W. D. Lavers (Y-12)
18. A M Weinberg
19. E. H. Taylor
20. E. J. Murphy
21 E. D. Shipley
22. J. H. Frye, Jr.
23. F. C. VonderLage
24. R. C. Briant
25. J A. Swartout
26 S. C. Lind
27. F L Steahly
28. A. H. Snell
29. A. Holla[redacted]
30. M. T. Ke[redacted]
31. K. [redacted] Mo[redacted]
32. J S Fe[redacted]
33. A. S. [redacted]
34. G. S. [redacted]
35. [redacted]
36. [redacted]
37. [redacted]
38. E. M. King
39. C. B. Ellis
40. W. H. Bridges
41. A. G. H. Andersen
42. L. K. Jetter
43. E. J. Boyle
44. W. D. Manly
45. C. D. Susano
46. W. W. Parkinson
47. R. J. Gray
48. B. S. Borie
49. C. D. Smith
50. D. E. Hamby
51. E. E. Stansbury
52. G. P. Smith
53. [redacted]
54. [redacted]
55. R. S. [redacted]
56. R. E. [redacted]
57. [redacted]vin
58. [redacted]tterton, Jr.
59. [redacted]lliams
60. [redacted]
61. [redacted]
62. L. A. Abrams
63. R. B. Day
64. T. W. Fulton
65. F. W Drosten
66. R. B. Oliver
67. P. Patriarca
68. J. T. Howe
69 T. H. Blewitt
70. W. E. Taylor
71. J. H. Crawford, Jr.
72. A. F. Cohen
73. J. C. Wilson
74 H. W. Savage
75-76. Central Files (OP)

EXTERNAL

77-79 [redacted], Oak Ridge
80-87. [redacted]
88-95. [redacted]
[redacted]
[redacted]
97-100. Brookhaven National Laboratory
101-104. Carbide and Carbon Chemicals Company (Y-12)
105-106. Knolls Atomic Power Laboratory
107-108. General Electric Company, Richland
109. Hanford Directed Operations
110-113. Los Alamos
114. Massachusetts Institute of Technology (Kaufmann)
115-116. New York Operations Office
117. Patent Branch, Washington
118. Savannah River Operations Office, Wilmington
119-133. Technical Information Branch, ORE
134-137. University of California Radiation Laboratory

[redacted]

Other Oak Ridge National Laboratory reports in this series are as follows:

Period Ending March 1, 1948	ORNL 28
Period Ending May 31, 1948	ORNL 69
Period Ending July 31, 1949	ORNL 407
Period Ending October 31, 1949	ORNL 511
Period Ending January 31, 1950	ORNL 583
Period Ending April 30, 1950	ORNL 754
Period Ending July 31, 1950	ORNL 827
Period Ending October 31, 1950	ORNL 910
Period Ending January 31, 1951	ORNL 987

[redacted]

TABLE OF CONTENTS

SUMMARY 9

1. THORIUM RESEARCH 11

Fabrication of Thorium 11
Drawing of Thorium 15
Extrusion Cladding of Thorium 17
Iodide-Process Thorium 17
Thermal Cycling of Thorium 20
Welding of Thorium 25

2. ANP PROGRAM 30

Liquid-Metal Corrosion Testing, Static 30
Static tests 30
Revision of static corrosion testing technique 30
Static corrosion test data 30
Liquid-Metal Corrosion Testing, Dynamic 34
Thermal convection loops 34
Cleaning procedures 51
Forced circulation loops 52
Powder Metallurgy 52
Fuel element fabrication 52
Mechanically formed matrix 52
Sintering and bonding a loose powder 54
Hot-rolled clad fuel plates 56
Cladding beryllium oxide 56
Compatibility tests of potential fuel element materials 61
Mechanical Testing 66
Welding Laboratory 67
Welding of inconel 67
Welding of refractory elements 70
Physical Chemistry of Liquid Metals 70
Interaction in presence of air 72
Interaction in presence of hydrogen 72

[redacted]

3. MTR FUEL UNITS 75

4. X-RAY LABORATORY 76

Effect of Precipitation in Copper-Beryllium Alloys 76

Hot-Laboratory Spectrometer Design 76

Room-Temperature Recovery in Copper 76

5. SERVICE WORK 81

Rolling Mill Section 81

ANP disks 81

Boral sheet 81

Spacer rod 81

KAPL washers 82

X-Ray Laboratory 82

Powder Metallurgy Section 82

LIST OF TABLES

1.1	Record of Thorium Extrusion	12
1.2	Thermal Cycling of Annealed Thorium and γ-Transformed Uranium in Na-K Between 100 and 500°C	24
1.3	Thorium and Uranium Bars Cycled Between 100 and 500°C in Na-K for 500 Cycles	27
1.4	Tensile Tests on Thorium Welds	29
2.1	Stainless Steels and Alloys Exposed to Lithium for 400 hr at 1000°C	37
2.2	Materials Tested in Lithium 400 hr at 1000°C	38
2.3	Corrosion and Operation Data of Thermal Convection Loops Containing Sodium	42
2.4	Corrosion and Operation Data of Thermal Convection Loops Containing Lead	44
2.5	Loose Powder Sintering and Bonding	55
2.6	Metal Spray Coating of Ceramic Base	63
2.7	Compatibility of Possible High-Temperature Reactor Constituents	65

LIST OF FIGURES

1.1	Thorium Tubing	16
1.2	Extruded Thorium Tubing with Zirconium Liner	18
1.3	Macro Section of Extruded Thorium Tubing with Zirconium Liner	19
1.4	Isothermal Recrystallization Curves for Iodide Thorium	21
1.5	Broken Tensile Test Specimens of Iodide Thorium	22
1.6	Specimens of Annealed Thorium and γ-Transformed Uranium After 906 Cycles in Na-K Between 100 and 500°C	23
1.7	Specimens Thermally Cycled in Na-K for 500 Cycles Between 100 and 500°C	26
2.1	Static Corrosion Testing — Capsulating and Tabulating Technique	31
2.2	Molybdenum Exposed to Sodium Containing Silicon	32
2.3	Molybdenum Exposed to Sodium	33
2.4	Hastalloys Exposed to Sodium	35
2.5	Comparison of Decarburized and "As Received" Inconel	36
2.6	Thermal Convection Loop — Old Design	40
2.7	Thermal Convection Loop — New Design	40
2.8	Weld Crevice in 316 Stainless Steel Loop	41
2.9	Oxide Inclusions in Weld Metal of 304 Stainless Steel Loop	41
2.10	Intergranular Attack Near the Weld of Nickel Loop	46
2.11	Pipe Sample from Nickel Loop Not Adjacent to Weld Zone	46
2.12	Mass Transfer Material in Cold Zone of Nickel Loop	47
2.13	Micro Section of Fig. 2.12	47
2.14	Intergranular Attack Near the Weld in 316 Stainless Steel Loop (No. 1)	48
2.15	Intergranular Attack Near the Weld in 316 Stainless Steel Loop (No. 16)	48
2.16	Intergranular Attack in Inconel Loop	50
2.17	Attack on External Surface of Nickel Loop	50
2.18	Perforations in Hard Brass Sheet	53

2.19	Effect of Stainless Steel Particle Size on UO_2 Distribution	57
2.20	Effect of Iron Particle Size on UO_2 Distribution	58
2.21	Double Clad, Pressed, Hot Rolled 302 Stainless Steel—UO_2 Compact — Etched and Unetched	59
2.22	Double Clad, Pressed, Hot Rolled Fe-UO_2 Compact — Etched and Unetched	60
2.23	BeO Sprayed Metal Interfaces	62
2.24	Tensile Test Jig	68
2.25	Cross-Section of Inconel Tube-to-Header Manual Inert Arc Weld	69
2.26	Cross-Section of Inconel Tube-to-Header Inert "Cone-Arc" Weld	71
2.27	Stereographic Projection of the Action of Liquid Mercury on a Copper Single Crystal Sphere in Air	73
2.28	Stereographic Projection of the Action of Liquid Mercury on a Copper Single Crystal Sphere in Hydrogen	73
2.29	Action of Mercury on a Single Crystal Sphere	74
4.1	Powder Pattern of Copper Sample	77
4.2	Results of Analysis of Distortions Normal to (331) Planes	79

SUMMARY

Experience thus far gained in extruding rods and tubing of thorium indicates that fabrication by extrusion is completely feasible. The extrusion die design and materials present the greatest problems at present because of the peculiar flow of thorium during extrusion and the high erosion rate. Thorium tubing clad inside with zirconium has been extruded satisfactorily. Work is continuing in order to obtain better surfaces and uniformity of cladding. The thermal cycling of thorium and uranium in Na-K has shown no real deformation of the thorium, but oxide scale formation with significant penetration did occur. An investigation on the welding of thorium has been started, and successful butt, edge, and lap welds have been made, using Heliarc techniques.

The static corrosion testing of constructional materials in a liquid-metal environment has continued. Work has started on the corrosion testing of various materials exposed to fused salts.

Dynamic corrosion testing using thermal convection loops containing sodium, lead, and lithium is being carried on jointly with the Experimental Engineering Section of the ANP Division. Stainless steel types 347, 321, and 310; inconel; and Haynes Alloy 25 displayed very little attack by sodium in 1000 hr at 1500°C. The welds are still the vulnerable areas, and various welding techniques need investigation to determine the best way to eliminate this source of failure.

Work on the fabrication of solid type fuel elements for high-temperature reactors is progressing. New types of perforated or mechanically deformed metal plates which can be loaded with UO_2 and clad are being considered. The pressed and clad type in which the UO_2 and a metal powder are pressed and then clad by hot rolling shows good continuous metallic network even up to 50% UO_2, and good bonding to the cladding material can be obtained. The spray coating of a metal surface onto massive beryllium oxide is being attempted; however, evaluation of the bond is difficult. The differences in thermal expansion between the BeO and the metal have led to the consideration of coating with some of the more refractory metals.

The Welding Laboratory is engaged in a program to develop suitable techniques for welding inconel tubing of small diameter to headers. Thus far manual inert-arc welding has been used, but equipment is being assembled to operate a semiautomatic cone-arc apparatus.

Recovery in copper at room temperature is being investigated by X-ray methods. An analysis of the (331) line in the copper pattern indicates that in copper filings recovery is complete in about one month.

1. THORIUM RESEARCH

FABRICATION OF THORIUM

Investigation of extrusion variables has been continued to permit satisfactory extrusion of rods and tubing of thorium. The only evaluation of extrusions at present is the surface quality as observed by visual inspection, and, by this criterion, all the extrusions have produced relatively good material. However, samples have been taken from each extrusion to make tensile test and creep specimens and at various points along the length of the extrusion for chemical analysis and for metallographic examination. The variables that have been investigated are billet temperature, extrusion rate, reduction ratio, lubrication, die design, and die materials. In so far as possible, all variables except the one under consideration were maintained constant while normal extrusion procedure was followed as outlined below.

The bare billets are heated in a salt bath (Houghton's Liquid Heat N.D.) for approximately 1 hr and manually transferred to the container of a 700-ton Lake Erie extrusion press. A graphite dummy block is placed behind the billet to remove the end of the extrusion from the die. A steel dummy block follows the graphite and the entire assembly is pushed with the ram. A water-quenching jig has been added to the press to quench the hot extruded rod or tube as it leaves the die and prevent excessive oxidation. This jig consists of two concentric pipes welded together to form an annulus which supplies high-pressure water through 1/8-in.-diameter holes in the inner pipe to quench the extrusion. The jig is bolted to the back of the die holder in order to begin quenching the extrusion approximately 18 in. behind the die.

A record of the extrusions is shown in Table 1.1. The variables are discussed individually below.

Billet Temperature. The billet temperature was varied from 950 down to 700°C. There was practically no visual difference in the surface of the 1-in. rods extruded in this temperature range. However, the graphite dummy block had a greater tendency to feed into the extruded rod during the 700°C extrusion. Lower temperature extrusions were not attempted partly because of

TABLE 1.1

Record of Thorium Extrusion

BILLET			EXTRUSION				
No.	SIZE (in.)	TEMPERATURE (°C)	SIZE (in.)	REDUCTION RATIO	EXTRUSION RATE (ft/min)	DIE TYPE	REMARKS
	2-15/16	925	1	9/1		Shear	Good
	2-15/16 × 3½ × ½	950	1 × 3/8	10 22/1	27	Shear	Good extrusion but hole slightly eccentric
	2-15/16 × 3½	950	1	8 93/1		Shear	Partially extruded to check flow pattern
	2-7/8 × 4	950	1	8.93/1		Shear	Glass bubble on surface rough (glass lubricant)
A229A	4 × 7½	910	2½	2 6/1		Shear, cast iron ring	Ring came through die (cast iron ring to simulate bell die)
A229B	4 × 7½	920	2½	2 6/1	7.8	Shear, tool steel ring	Extrusion appeared too hot
A221	4 × 8½	875	2½	2.6/1	7.85	Shear	Good
A228A	4 × 7¼	850	2½	2.6/1	8.0	Shear	Billet cracked
A219	4 × -	850	2½	2.6/1	10.0	Shear	Good
A230	4 × -	850	2½	2.6/1	9.0	Shear	Good
A230B	4 × 6-7/8	850	2½	2.6/1	8.0	Shear	Good
A231B	3 × 8	800	1	9/1	32.5	Shear	Good; die has small cracks
A231A	3 × 8	800	1	9/1	31	Shear	Good
A231C½	3 × 4	700	1	9/1	33.8	Shear	Extrusion has graphite forced into it
A231C½	3 × 4½	700	1	9/1	35.4	Shear	Extrusion has graphite forced into it
A234A	3 × 4-3/8	850	3/4	16/1	22.0	Shear	Die washed out in extrusion
234A	3 × 4½	850	½	36/1	90.0	Shear	Die washed out in extrusion
227A	3 × 4-7/16	850	½	36/1	21.4	Shear	Fair
227A1	3 × 4-3/8	850	½	36/1		Shear	Rod stuck in trough and coiled up
A228B	4 × 7¼	840	2½	2 6/1	9.0	Shear, tool steel ring	Ring cracked; showed no signs of washing
239B	3 × 6	850	1	9/1	>400	Shear	Good insert cracked slightly
239A	3 × 6	850	1	9/1	>400	Shear	Good
239D1	3 × 4-7/8	850	1	9/1	565	Shear	Good
239D2	3 × 4-7/8	850	1	9/1	32.7	Shear	Good
223A	3 × 4-7/8	850	1	9/1	32.25	Shear	Good

TABLE 1.1 (Cont'd)

NO.	BILLET SIZE (in.)	BILLET TEMPERATURE (°C)	EXTRUSION SIZE (in.)	EXTRUSION REDUCTION RATIO	EXTRUSION RATE (ft/min)	DIE TYPE	REMARKS
222C	3 × 4	850	1	9/1	562.5	Shear	Good
239C1	3 × 4	850	1	9/1	2.1	Shear	Good
239C2	3 × 4	850	1	9/1	2.7	Shear	Good
234B1	3 × 4½ × 9/16	850	1	10.08/1	3.02	Shear	Good
234C1	3 × 4½ × 11/16	780	7/8	22.73/1	90	Bell	Excellent extrusion
234C2	3 × 4½ × 9/16	800	7/8	14.67/1	50	Shear	
225C1	3 × 4 × 11/16	900	7/8	13.64/1	41.08	Shear	
225C2	3 × 4 × 7/16	900	7/8 × 3/8	14/1	35	Shear	The mandrel broke from tension after extrusion of 6 in. of tube; remainder of extrusion good
225B1	3 × 4 × 9/16	800	7/8 × 1/2	17/1	30	Shear	Hole appears to be eccentric
225B	3 × 4-1/8 × 11/16	840	7/8 × 5/8	22/1	66	Bell	Several cracks found in insert after extrusion
222C	3 × 4 × 13/16	840	7/8 × 3/4	41.5/1		Bell	Reduction too great for billet temperature
223A	3 × 4 × 13/16	1000	7/8 × 3/4	41.5/1		Bell	End of mandrel broke from tension; after extruding 6 ft of tubing die was undersize and mandrel oversize (press stalled); 1/32-in. wall
241-1	3 × 4 × 7/16	850	7/8 × 3/8	14/1	60	Bell	1- by 1/16-in. core of zirconium in billet; temperature too high for extrusion of zirconium core; mandrel broke
241-2	3 × 3½ × 9/16	725	7/8 × 1/2	17/1	61	Bell	1- by 9/16-in. core of zirconium was welded into thorium billet; thorium and zirconium appeared to have good bond; some die marks visible on tube

this tendency and partly because the press was operating at near its maximum pressure capacity. It is planned to extend the work to higher temperatures, probably 1000 and 1100°C.

Extrusion Rate. The effect of extrusion rate was investigated by extruding 1-in.-diameter rods at speeds varying from 4 to 450 ft/min. There was no difference apparent in the quality of extrusion over the entire range of rates. A speed of about 50 ft/min was adopted for the remainder of the extrusion work because it was convenient and allowed a suitable period of time for water-quenching the extrusion.

Reduction Ratio. The effect of reduction ratio has been investigated by extruding billets 3 and 4 in. in diameter into rods and tubing of various sizes. The reduction ratios varied from 2.5/1 to 36/1, and all extrusions produced rods with a good surface quality. Since this was the only criterion at this stage, it was concluded that the quality of extrusion is independent of reduction ratio within the range investigated.

Lubrication. Various lubricants have been used in the extrusion of thorium. Glasses with low melting points have been used, but they proved to be unsuccessful because of chilling during extrusion and then scoring the surface and giving an unsatisfactory surface in general. Lampblack—machine oil lubricant was tried, but results were improved by substitution of beeswax for the oil. Later, the practice of mixing flake graphite and sodium silicate to form a thick paste which was applied to the cold stem and die gave much better results. This lubricant was used for the latest extrusions. Other lubricants are being obtained for further study.

Die Design. Prior experience and the ease of fabrication and availability of flat-faced dies dictated their use for most of the early work on extrusion. These dies were either made from a solid steel forging or contained an insert in the nose of the die to take the wear during extrusion. Dies of the insert type are being used to investigate the effect of die design since the inserts are relatively cheap from the standpoint of fabrication, and a material that is satisfactory for the die body does not appear to offer a satisfactory working surface. The working part of the die, made of a suitable material and to a desired shape, is inserted in a nose of the die body. Variations of the shear type die are being studied by using various shapes of bell die inserts. One such die, having a 30° face angle with a ½-in. throat radius

and ¼-in. bearing, produced an excellent tube. A longitudinal section of this extrusion and a piece of the tubing produced are shown in Fig. 1.1.

Die and Mandrel Materials. Die and mandrel materials present the greatest problem at present. The normal hot-work die steels such as Allegheny-Ludlum's Potomac, Latrobe's C.H.W. and L.P.D., and Braeburn's T-Alloy have not made one extrusion without failing. This problem is complicated by the peculiar flow of thorium during extrusion, which was found on the first extrusions: the metal flowed across the face of the flat-faced shear type die rather than through the billet as is the case in most other metals. This type of flow lends itself somewhat better to a bell type die than to a shear type owing to the erosion of the shape orifice at the entrance of the throat in a shear die. The erosion experienced during the test of some die materials has been sufficient to produce a resemblance of a bell die in a shear die. However, bell dies of some materials have been unsuccessful. In the case of one hot-work die steel the throat of the die was washed out and the die diameter was made considerably larger. Because of this erosion insert dies were made of a stellite type material and a high-cobalt, 18-4-1, steel. These materials appear to withstand the erosion equally well, but they are both susceptible to cracking. Some of the stellite type (Doss Steel Research Company 3130 alloy) inserts have cracked considerably during the first extrusion. Modifications of these two materials are being investigated in an attempt to find a tough material sufficiently hard to withstand the erosion. Experience with the mandrels is about the same as with the dies. The steel mandrel becomes soft, and, in the case of one stem 3/8 in. in diameter, it actually failed in tension. A stellite type (Doss Steel Research Company 2115 alloy) failed with a brittle fracture on the first extrusion.

DRAWING OF THORIUM

Very little work has been done on drawing of thorium. One short length of rod was drawn from 0.500 to 0.451 in. in diameter by coating with flake graphite, pulverized mica, and sodium silicate and heating to 300°C. Dies and samples of various lubricants are being procured for further study.

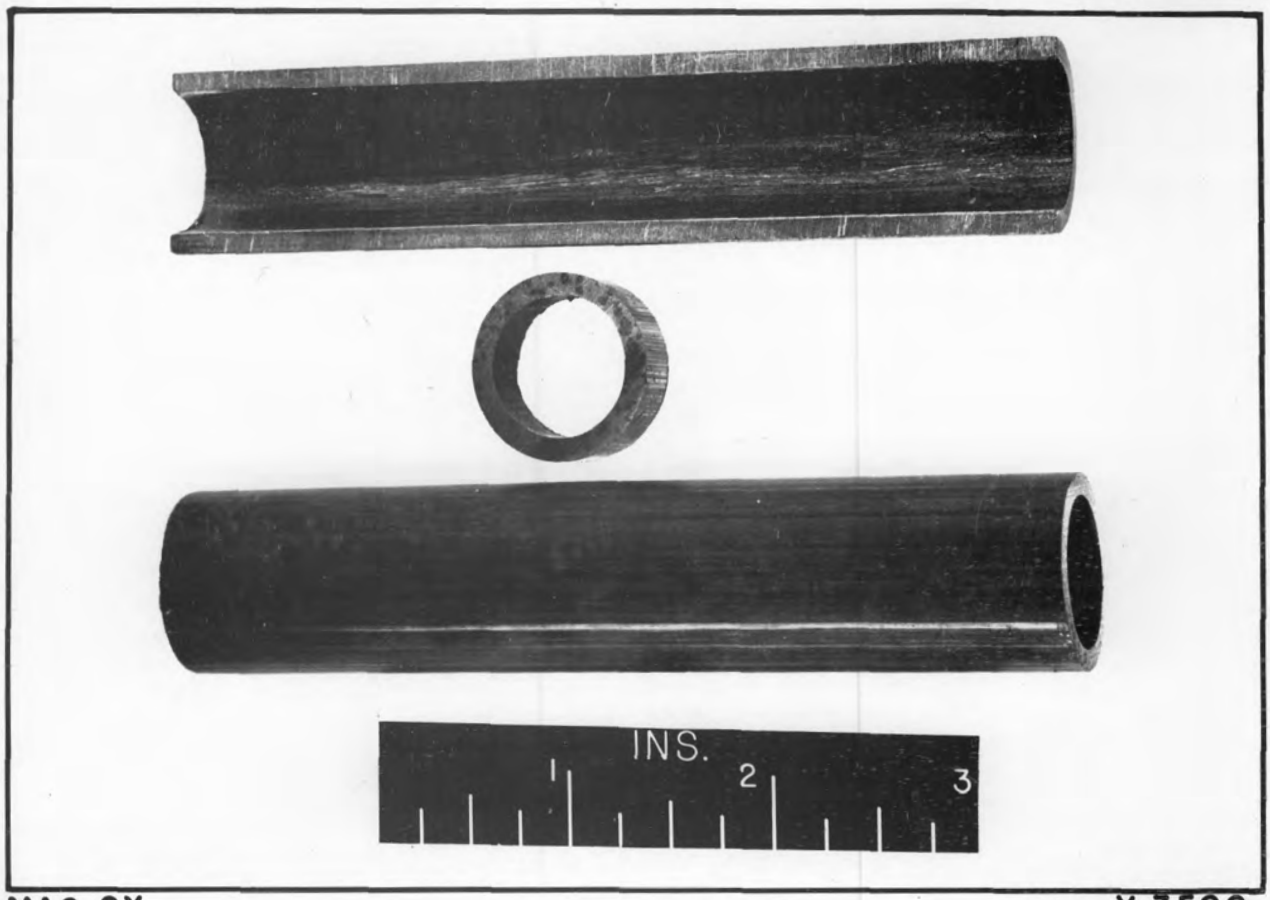

MAG. 2X Y-3500

THORIUM TUBING- 7/8" O.D. X 5/8" I.D

EXTRUSION CONDITIONS:

REDUCTION RATIO — 25/1
EXTRUSION RATE — APPROXIMATELY 90 ft/min.
BILLET TEMPERATURE — 780°C
HEATING — 1 HOUR 20 MINUTES IN HOUGHTON'S "LIQUID HEAT ND."
DIE — DOSS "3130 ALLOY" INSERT 30° BEVEL PREHEATED TO 1200°F
MANDREL — "ELECTRITE VANADIUM" FORGED PREHEATED TO 1000°F
LUBRICANT — FLAKE GRAPHITE + SODIUM SILICATE
QUENCH — COLD WATER

FIG. 1.1

EXTRUSION CLADDING OF THORIUM

An extrusion of a duplex thorium-zirconium billet was made at a temperature of 725°C with a reduction ratio of 16/1 to produce a thorium tube of 7/8 in. O.D. and ½ in. I.D. with an inside cladding of about 0.020 in. of zirconium. The zirconium cladding was fairly uniform, and the tubing had a fair surface on both the inner and outer side. A back bend of the tubing passed through approximately 200° before the liner of zirconium broke, and the broken ends of the cladding could not be stripped mechanically from the thorium. Photomicrographs of the tube at the thorium-zirconium interface are shown in Figs. 1.2*a* and *c*. There was some diffusion between the two metals and a metallurgical bond was apparently obtained. The sharp line of demarcation between the thorium and zirconium was due to preferential attack during polishing and etching and does not represent a void. It may be seen from Figs. 1.2*b* and *d* that the zirconium cladding is slightly thicker and more uniform at the leading end of the extrusion than at the trailing end. Macro sections of the duplex tubing at both the leading and the trailing end of the extrusion are shown in Fig. 1.3. The zirconium appears to be metallurgically bonded very satisfactorily, and it seems probable that the conditions of temperature and reduction used in this extrusion are sufficient to ensure bonding. Further work is needed to improve the uniformity of cladding and obtain more satisfactory surfaces.

IODIDE-PROCESS THORIUM

Thorium prepared by the thermal decomposition of thorium tetraiodide on a hot tungsten filament was obtained from Battelle Memorial Institute for a study of the properties of high-purity metal. Spectrographic analysis of the material showed it to be spectrographically pure except for a very faint trace of calcium. Chemical analysis revealed the following impurities: oxygen, 0.012%, hydrogen, 0.0002%, and carbon 0.05%.

In order to keep the contamination to a minimum, the metal was melted in a vacuum-arc furnace, using the crystal bar thorium as a consumable electrode. The melted metal had a Vickers hardness number of approximately 40. By way of comparison, Ames metal has a hardness of about 85 Vickers. The melted ingot

NOT CLASSIFIED
Y-4203

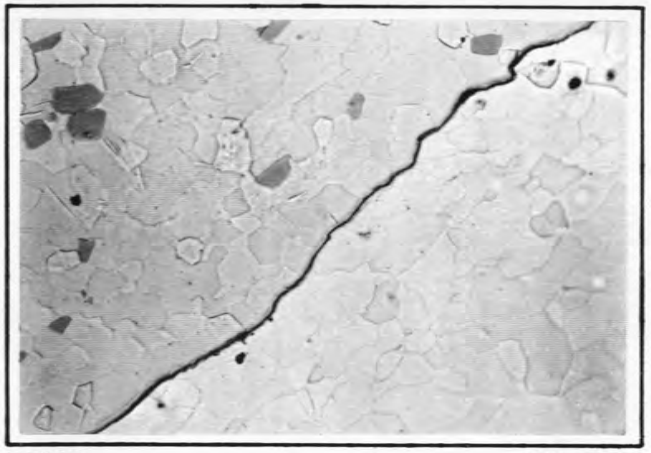

Y-3957 MAG. 1000 X

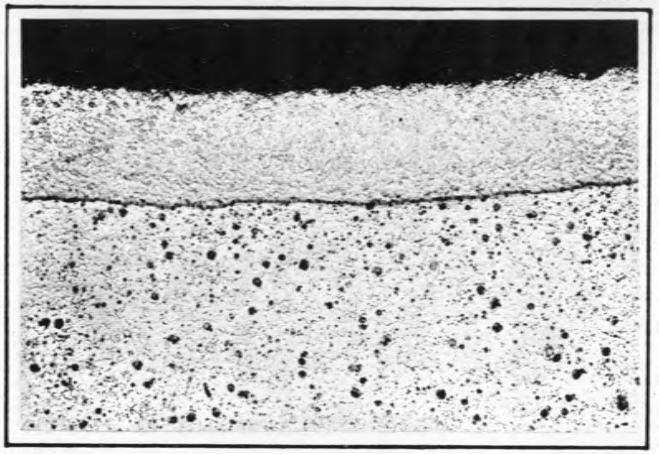

Y-3956 MAG. 100X

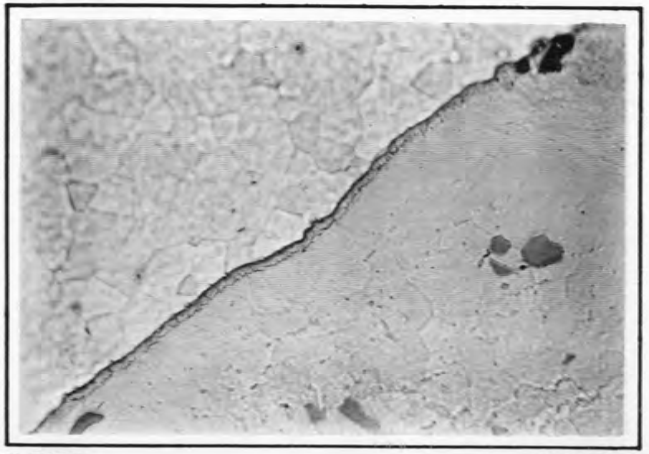

Y-3959 MAG. 1000X

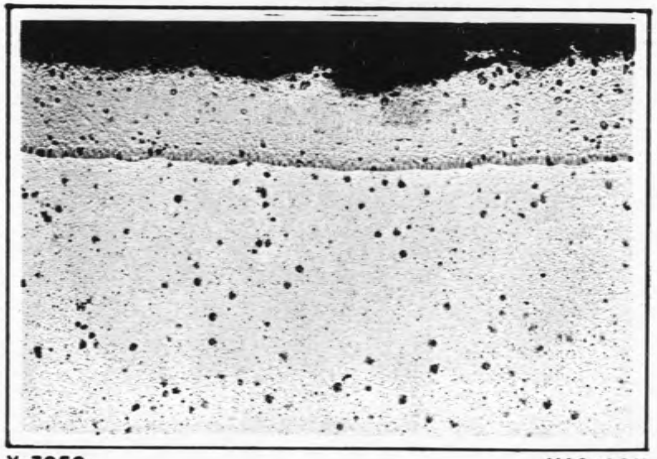

Y-3958 MAG. 100 X

EXTRUDED THORIUM TUBING WITH ZIRCONIUM LINER

FIG. I.2

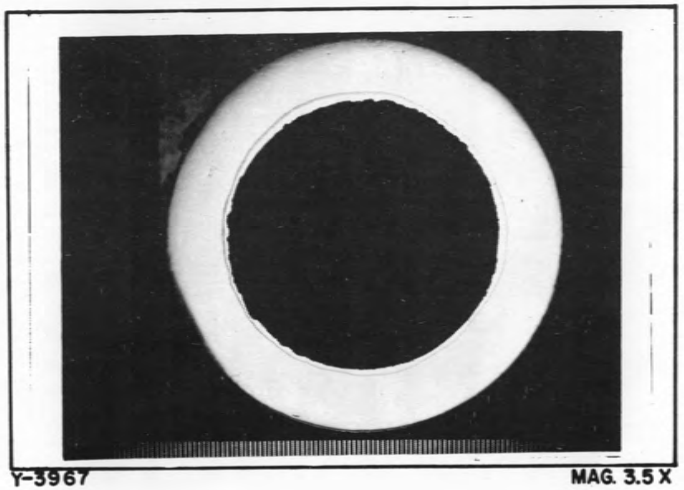

Y-3967 MAG. 3.5 X

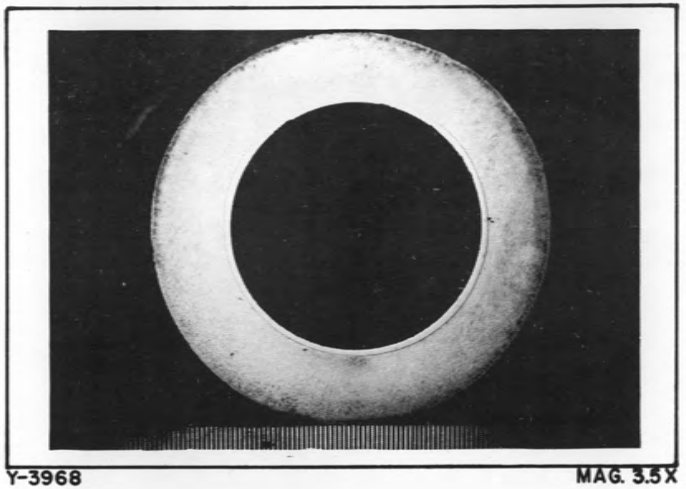

Y-3968 MAG. 3.5 X

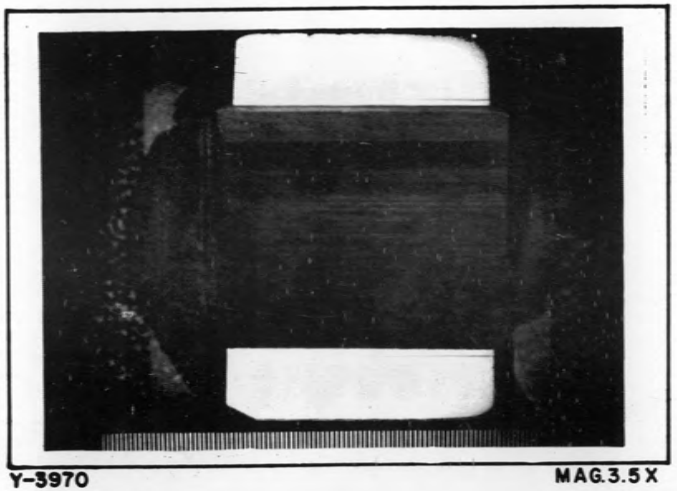

Y-3970 MAG. 3.5 X

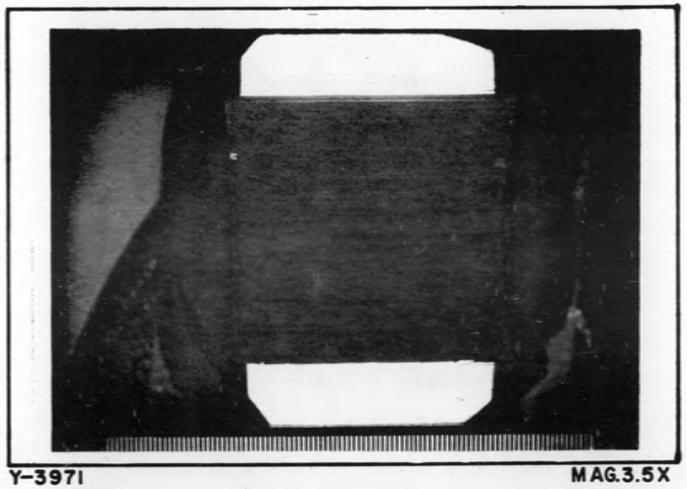

Y-3971 MAG. 3.5 X

MACRO SECTION OF EXTRUDED THORIUM TUBING WITH ZIRCONIUM LINER

FIG. 1.3

was cold-rolled for 80% reduction, and the rolled sheet was cut into specimens for recrystallization studies. A work-hardening curve, obtained while rolling the ingot, was similar to those previously reported for thorium, i.e., the metal reached very nearly its maximum hardness at about 5% reduction. The material after 80% reduction was found to have a hardness of 65 Vickers. The metal was heated at 550°C for various lengths of time with very little, if any, recovery taking place. The thorium failed to recrystallize after being held at 550°C for 1 hr. However, isothermal recrystallizations were obtained at 650 and 700°C. These curves are shown in Fig. 1.4. The material was fully recrystallized in each case after about 5 min at temperature.

One complete melt of the iodide-process thorium was rolled into a bar and machined into a round tensile test specimen 0.357 in. in diameter. The specimen was annealed after machining.

In the tensile test the modulus of elasticity was measured with SR-4 strain gauges and found to be 10,000,000 psi. The ultimate strength was 22,680 psi. The specimen was extremely ductile, having a reduction in area of about 95%. Percent elongation could not be measured, since the specimen broke outside the gauge marks. Figures 1.5*a* and *b* are photographs of the broken test specimen. Note the triangular shape of the fracture, and the rather abrupt way in which the specimen necked down.

THERMAL CYCLING OF THORIUM

Specimens of thorium rod were cycled in Na-K between 100 and 500°C as described in a previous report (ORNL-987). The first set of samples, annealed thorium, was cycled for a total of 1000 cycles. The only significant change was a consistent weight loss during cycling. The dimensions increased slightly in all directions owing to a scale which formed on the bars and which was shown by X-ray analysis to be pure ThO_2. However, no real deformation of the thorium bars was noted. The furnace was charged with Na-K which had not been purified, but a protective atmosphere of purified argon was maintained at all times. A sample of gamma-transformed uranium was cycled along with the thorium and showed the warping and surface roughening which is characteristic of this material. The data for both the thorium and uranium are shown in Table 1.2. The specimens after having been cycled for 906 cycles are shown in Fig. 1.6.

[redacted]

DWG.11751

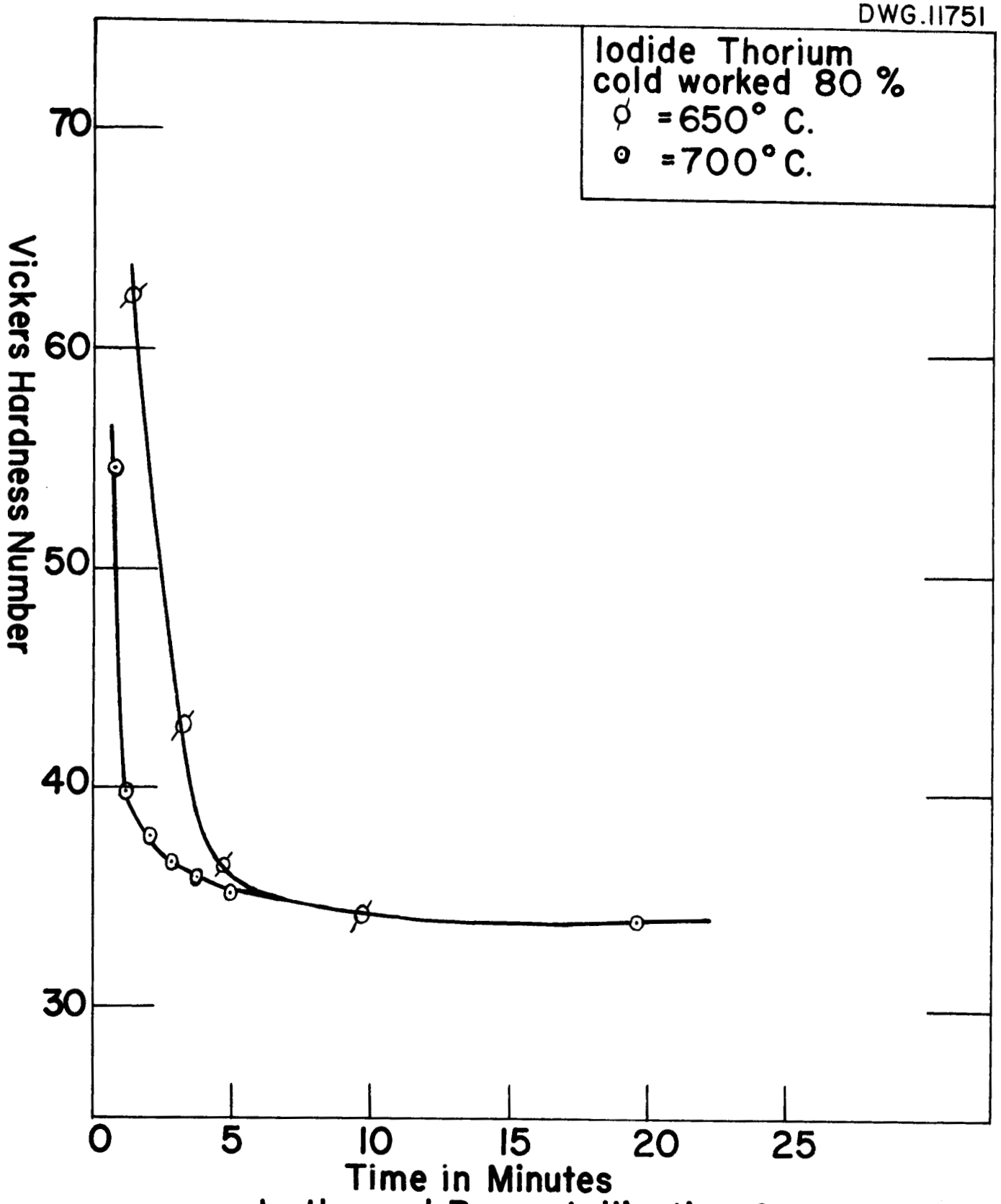

Isothermal Recrystallization Curves For Iodide Thorium

FIG. 1.4

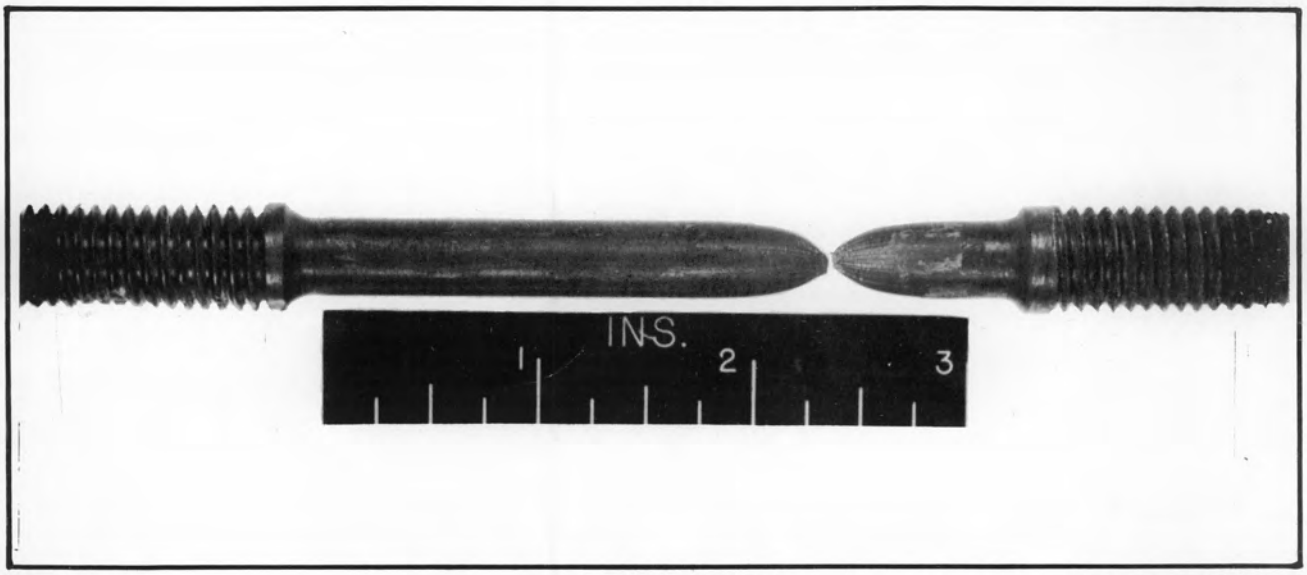

Y-3711 A. LONG. VIEW SLIGHT MAG.

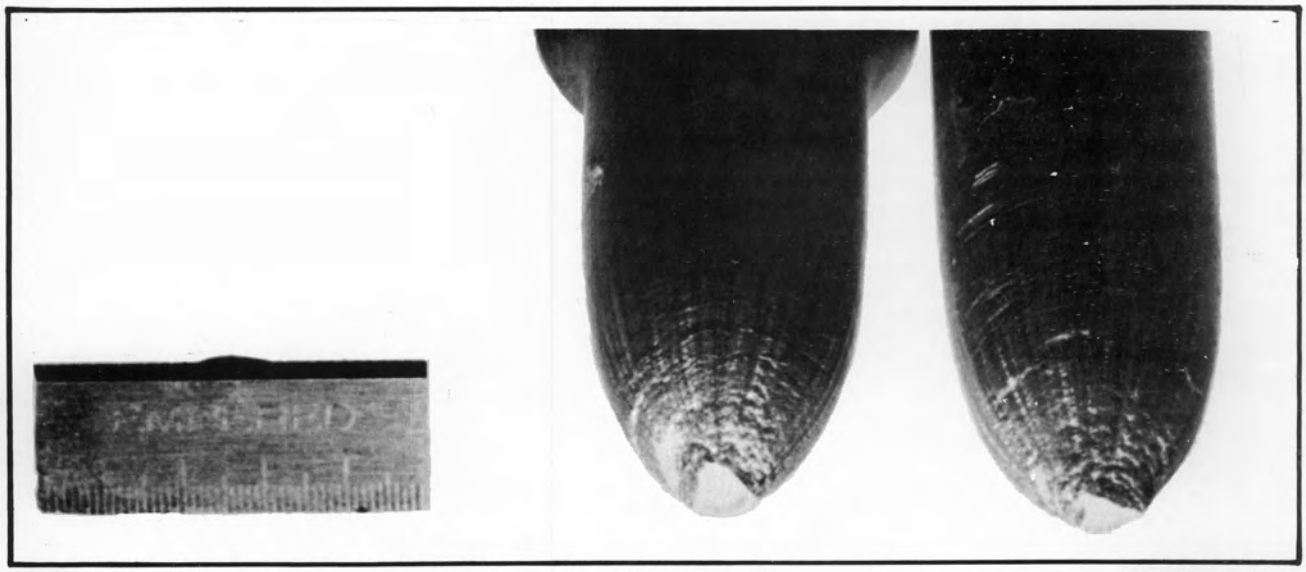

Y-3712 B. END VIEW MAG. 2X

BROKEN TENSILE TEST SPECIMENS OF IODIDE THORIUM

FIG. 1.5

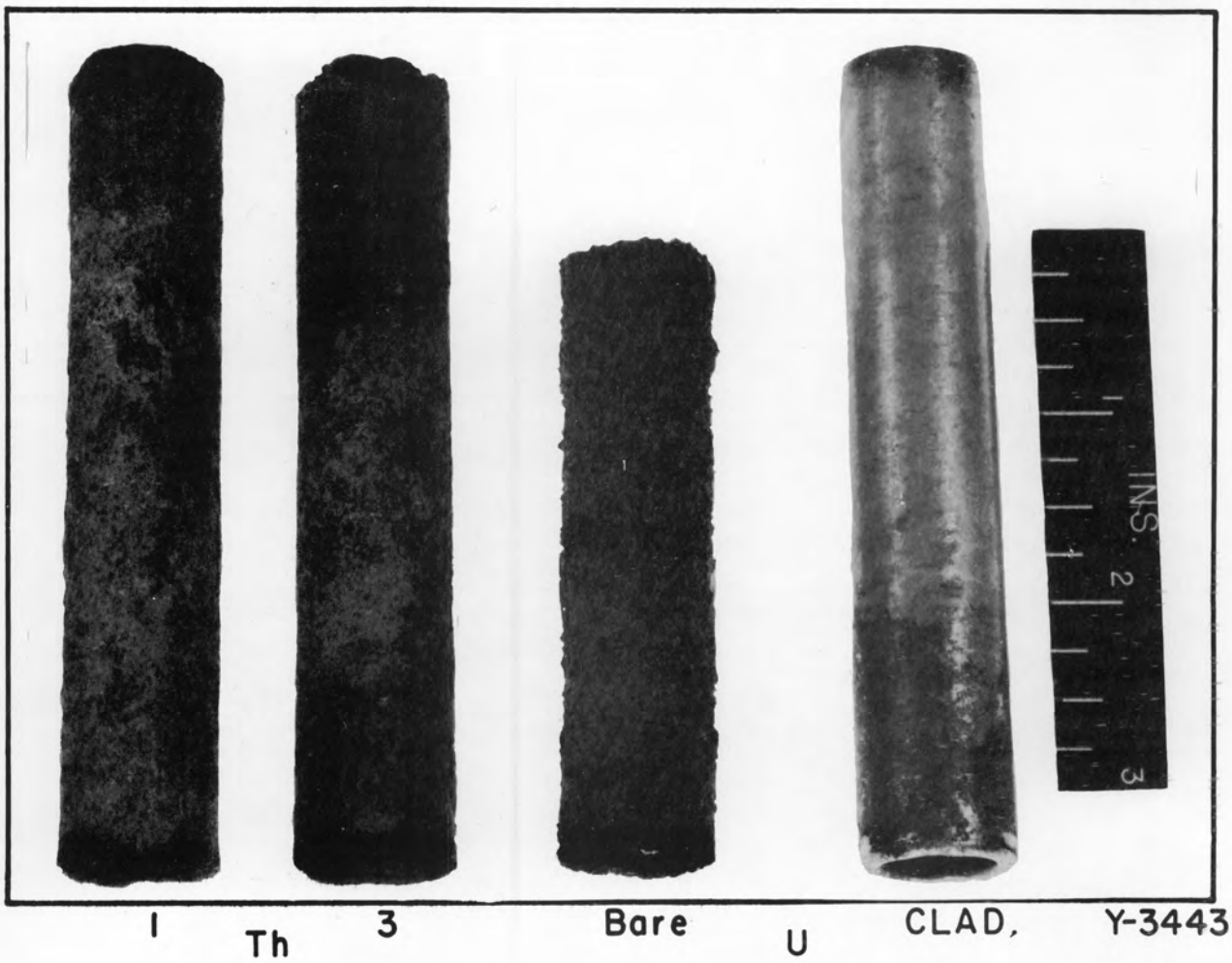

SPECIMENS OF ANNEALED THORIUM AND γ TRANSFORMED URANIUM AFTER 906 CYCLES IN NaK BETWEEN 100°C–500°C.

FIG. 1.6

TABLE 1.2

Thermal Cycling of Annealed Thorium and γ-Transformed Uranium in Na-K Between 100 and 500°C

	ORIGINAL	100 CYCLES	300 CYCLES	400 CYCLES	500 CYCLES	600 CYCLES	700 CYCLES	800 CYCLES	900 CYCLES	1000 CYCLES
Thorium No. 1										
Length, l (in.)	4.012	4.026	4.051	4.061	4.075	4.091	4.091	4.097	4.110	4.099
Diameter, d (in.)	0.750	0.752	0.760	0.757	0.772	0.763	0.763	0.769	0.769	0.768
Weight, W (g)	333.876		334.133	330.965*	324.898	322.851	320.303	319.619	317.500	316.653
Δl		+0.014	+0.039	+0.049	+0.063	+0.079	+0.079	+0.085	+0.098	+0.087
Δd		+0.002	+0.010	+0.007	+0.022	+0.013	+0.013	+0.019	+0.019	+0.018
ΔW			+0.257	-2.911	-8.978	-11.025	-13.573	-14.257	-16.376	-17.223
Weight loss (%)			0.07	0.88	2.69	3.3	4.07	4.27	4.9	5.15
Thorium No. 2										
Length, l (in.)	4.005	4.021	4.043	4.048	4.064	4.081	4.080	4.069	4.103	4.102
Diameter, d (in.)	0.750	0.752	0.763	0.761	0.762	0.765	0.767	0.774	0.775	0.764
Weight, W (g)	333.876		334.350	330.470	327.405	325.585	323.696	322.813	316.370	313.901
Δl		+0.016	+0.038	+0.043	+0.059	+0.076	+0.075	+0.064	+0.098	+0.097
Δd		+0.002	+0.013	+0.011	+0.012	+0.015	+0.017	+0.024	+0.025	+0.014
ΔW			+0.474	-3.406	-6.471	-8.291	-10.180	-11.063	-17.506	-19.975
Weight loss (%)			+0.11	1.02	1.94	2.48	3.04	3.31	5.24	5.98
γ-Transformed Uranium										
Length, l (in.)	3.000	2.998	3.001	3.010	2.981	3.009	3.017	3.030	3.006	3.005
Diameter, d (in.)	0.755	0.761	0.775	0.783	0.770	0.771	0.775	0.783	0.771	0.780
Weight, W (g)	411.406		410.768	409.188	402.655	397.823	394.881	391.662	381.917	373.650
Δl		-0.002	+0.001	+0.010	-0.019	+0.009	+0.017	+0.030	+0.006	+0.005
Δd		+0.006	+0.020	+0.028	+0.015	+0.016	+0.020	+0.028	+0.016	+0.025
ΔW			-0.638	-2.218	-8.751	-13.583	-16.525	-19.744	-29.489	-37.756
Weight loss (%)			0.15	0.54	2.13	3.3	4.01	4.8	7.16	9.17

*Scale removed for identification.

The second set of specimens cycled was made up of the following: cold-rolled thorium, cold-swaged thorium, as-extruded (800°C) thorium, alpha-rolled uranium (bare), and alpha-rolled uranium (canned). At the end of 500 cycles the bare uranium specimen showed the normal growth of alpha-rolled material (approximately 20% elongation). The specimen which had been canned in the stainless steel tubing with a 0.030-in. wall thickness did not show appreciable elongation or any change in diameter. Thus it appears that the growth during cycling of alpha-rolled uranium may be restrained.

The thorium specimens showed no significant changes after 500 cycles between 100 and 500°C except for a 2 to 3% weight loss which also occurred in the annealed specimens. These specimens after 500 cycles are shown in Fig. 1.7. The data before cycling and after 500 cycles are shown in Table 1.3.

The oxidation of the specimens is evidently caused by oxides of sodium and potassium in the initial bath metal, which are reduced by thorium and uranium. This oxidation apparently penetrates the thorium fairly readily since the bars crumble and spall off at the ends, as may be seen in Figs. 1.6 and 1.7. On metallographic examination of the bar in cross-section an oxide gradient was found which extended practically to the center of the bar, thus verifying this penetration.

WELDING OF THORIUM

A study on welding of thorium has been started. In preliminary welding tests, using Ames thorium sheet, butt, edge, and lap welds were readily made in a helium atmosphere, using Heliarc-welding techniques.

Welding was done in a dry box, using Grade A tank helium as an inert gas. Prior to the welding the box was partially evacuated and allowed to refill with helium a few times to purge air from the box. Helium was fed through the torch continuously. Welds obtained were clean and bright, and had an excellent appearance. Brief experiments using argon through the torch, and using a helium torch in an air atmosphere, did not produce good welds.

Satisfactory welds using helium have been produced using both a-c and d-c straight-polarity arcs. All welds were made on thin sheets (up to 0.080 in. thick) and no filler rod was used. Butt welds were made without restraint

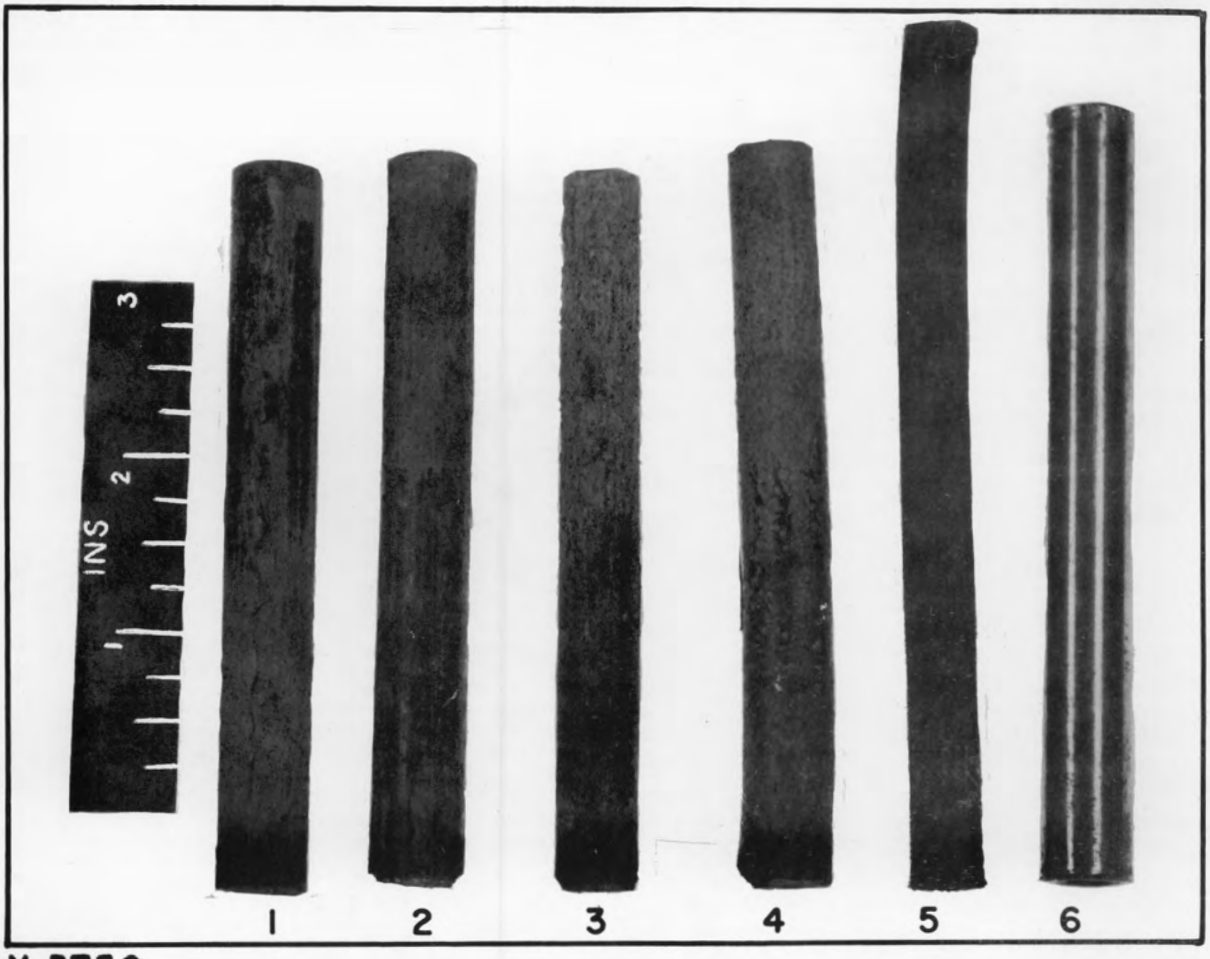

Y-3750

SPECIMENS THERMALLY CYCLED IN NaK FOR 500 CYCLES BETWEEN 100°C-500°C

1. COLD ROLLED THORIUM ROD.
2. COLD ROLLED THORIUM ROD.
3. COLD SWAGED THORIUM ROD.
4. AS EXTRUDED THORIUM ROD.
5. α ROLLED URANIUM.
6. α ROLLED URANIUM CANNED IN STEEL.

FIG. 1.7

TABLE 1.3

Thorium and Uranium Bars Cycled Between 100 and 500°C in Na-K for 500 Cycles

MATERIAL	TIME OF MEASUREMENT	LENGTH (in.)	DIAMETER (in.)	WEIGHT (g)
Annealed thorium	Before cycling	4.012	0.750	333.876
	After 500 cycles	4.075	0.772	324.898
	Change	+0.063	+0.022	-8.978
	% Change	1.57	2.93	2.69
Cold-rolled thorium	Before cycling	4.032	0.498	150.301
	After 500 cycles	4.034	0.498	145.960
	Change	+0.002	0.000	-4.341
	% Change	0.05	0.0	2.89
Cold-rolled thorium	Before cycling	4.009	0.497	148.776
	After 500 cycles	4.023	0.505	145.892
	Change	+0.014	+0.008	-2.884
	% Change	0.35	1.61	1.94
Cold-swaged thorium	Before cycling	3.981	0.440	114.615
	After 500 cycles	3.974	0.447	110.316
	Change	-0.007	+0.007	-4.299
	% Change	1.86	1.59	3.75
Thorium as extruded at 800°C	Before cycling	4.030	0.485	144.550
	After 500 cycles	4.106	0.495	140.405
	Change	+0.076	+0.010	-4.145
	% Change	1.88	2.06	2.87
Bare uranium	Before cycling	4.000	0.437	186.237
	After 500 cycles	4.785	0.404	175.681
	Change	+0.785	-0.033	-10.556
	% Change	19.62	7.53	5.67
Uranium in stainless steel can (can thickness 0.030 in.)	Before cycling	4.252	0.502	215.774
	After 500 cycles	4.275	0.501	215.178
	Change	+0.023	-0.001	-0.596
	% Change	0.54	0.2	0.17

since, when pieces were clamped while welding, cracks developed in the weld. When a second pass was made over the welded joint, cracking also developed.

Preliminary welds were tested by bending in a vise. Good welds could be bent from 30 to 90° before cracking, breaks usually occurring in the heat-affected zone.

Tensile tests were made on several butt-welded sheet-thorium specimens 6 in. long, 1 in. wide, and 0.040 or 0.080 in. thick. Specimens were sheared from the butt-welded sheet, discarding the cratered weld metal at the start and end of the weld. Tensile specimens were not machined, and the welded joints were slightly thicker than the base metal. All fractures occurred in the heat-affected base metal. Specimens were annealed prior to testing.

Data obtained from the tensile tests are shown in Table 1.4. It is apparent that the yield point and tensile strength of the specimens were not affected by the welding. The ductility of the welded specimens was somewhat lower than that of the specimens which contained no welds. However, ductility of the weld material is partly masked as a result of the slightly greater thickness at the weld. Some deformation of the weld metal did occur. This is shown by the reduction in width at the weld, which ranged from 5 to 8%. Reductions in width at the fractures ranged from 10 to 18%.

Hardness traverses across several welded joints have been made. In one series of tests weld metal was not appreciably harder than the base metal. In similar tests on a softer lot of thorium the hardness of the weld metal was somewhat greater than the hardness in the heat-affected zone. Further work is needed to define the effect of welding on the hardness of thorium.

Additional tensile tests will be made on specimens machined to remove the excess metal at the welds. Welding tests on heavier metal sections will be made, and tensile tests will be made on round specimens machined entirely from weld metal.

TABLE 1.4

Tensile Tests on Thorium Welds

SPECIMEN NO.	THICKNESS (in.)	YIELD POINT (psi)	ULTIMATE STRENGTH (psi)	ELONGATION, 2-in. GAUGE LENGTH (%)	REDUCTION* IN WIDTH AT FRACTURE (%)	REDUCTION* IN WIDTH AT WELD (%)
Blank 1	0.080	29,400	38,600		17.1	
Blank 2	0.080	29,400	38,500	44	18.1	
Weld 2B	0.080	29,400	39,000	34	17.4	5.0
Weld 3A	0.080	28,800	38,500	34	10.7	8.4
Weld 3B	0.080	29,900	38,100		10.9	7.3
Blank 1	0.042	30,600	38,000		15.4	
Blank 2	0.042	31,100	38,500	36	16.7	
Weld 1	0.042	30,000	38,600	36	10.0	6.2
Weld 2	0.042	30,000	39,000	32	9.5	6.6

*% reduction in width = (initial width - final width) ÷ initial width.

2. ANP PROGRAM

LIQUID-METAL CORROSION TESTING, STATIC

Static Tests. The testing of materials for the proposed ARE is being continued. Metals and alloys are being tested at varying exposure times and temperatures to determine possible saturation effects. The phenomenon of mass transfer is being studied, and tests made under conditions where mass transfer was observed using the capsulating technique have been compared with tests made in a two-component system in order to determine the type of attack encountered in the absence of a third component.

Preliminary corrosion tests have been made in $NaF-BeF_2-UF_4$ eutectic salt mixture for 100-hr periods at 1000°C. Complete metallographic data are not yet available but will be included in a subsequent progress report.

Revision of Static Corrosion Testing Technique. Complete transition to the two-component system containing sodium filtered to remove suspended oxides has not been fully accomplished as yet. The bath metal purification and filling devices have been constructed and installed and are being inspected. Initial tests on this apparatus will begin in the very near future.

Three-component tests have been discontinued, but those completed previously will be evaluated and reported. Until the filling apparatus is in operation, the samples will consist of open-end tubes, with bath metal inside, inserted into a safety pressure capsule and tested in an upright position. Figures 2.1*a* and *b* illustrate the former (capsulating) and proposed (tubulating) techniques, respectively, for conducting static liquid-metal corrosion tests.

Static Corrosion Test Data. *Sodium.* Several tests in sodium have been made to observe mass transfer. When silicon was added to the sodium in a molybdenum tube which contained a molybdenum sheet specimen, the silicon was observed to form a hard brittle plate, largely molybdenum disilicide, on the inside of the molybdenum crucible; almost the entire thin-sheet specimen of molybdenum had reacted (Fig. 2.2). In contrast, a molybdenum specimen tested in silicon-free sodium for 100 hr at 1000°C showed no weight change and no evidence of attack (Fig. 2.3). Two hastelloys, B and C, have been tested in

NOT CLASSIFIED
Y-4210

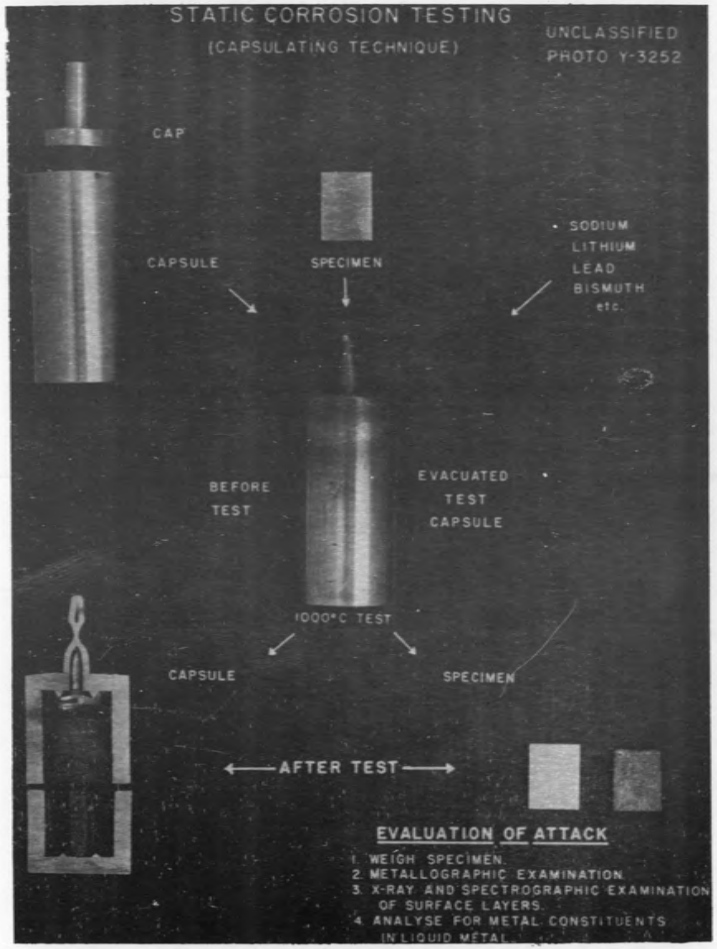

Y-3252

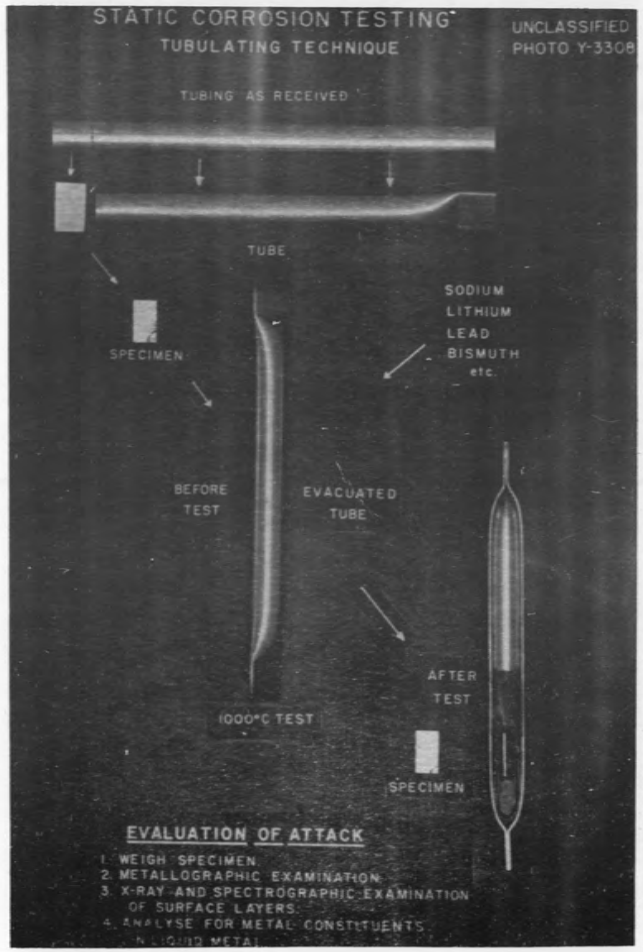

Y-3308

STATIC CORROSION TESTING

(CAPSULATING AND TUBULATING TECHNIQUE)

FIG. 2.1

NOT CLASSIFIED
Y-4200

ETCH: 0.5% OXALIC ACID Y-3552 MAG. 250X

MOLYBDENUM EXPOSED TO SODIUM CONTAINING SILICON FOR 100 HOURS AT 1500° F.

FIG. 2.2

NOT CLASSIFIED
Y-4201

ETCH: 0.5% OXALIC ACID Y-3756 MAG. 250X

MOLYBDENUM EXPOSED TO SODIUM FOR 100 HOURS AT 1000°C

FIG. 2.3

sodium for 40 hr at 1000°C. The hastelloy B test was a two-component type and the sodium had no apparent effect other than decarburization and possible precipitation of some angular grain boundary constituent in the decarburized region. Although the hastelloy C test was capsulated in nickel, no mass transfer was noted and the only visible attack was in the form of small shallow voids less than 0.001 in. deep (Fig. 2.4).

Lithium. Many alloys and elements have been tested in lithium for 400 hr at 1000°C using iron capsules. The metallographic results are summarized in Tables 2.1 and 2.2. Of the alloys tested, the lower-chromium ferritic stainless steels showed the best resistance to attack. Nickel and high-nickel alloys were severely attacked.

Lead. Several additional tests have been made with lead to check for mass-transfer effects, but the results of these tests are not yet available.

Fused Salt Solutions. The corrosive action of a low-melting fused salt solution of 10 mole % BeF_2, 68 mole % NaF, and 21 mole % UF_4 was tested for 100 hr at 1000°C on several of the austenitic stainless steels, one ferritic stainless steel, inconel, inconel X, nickel, hastelloy B, and iron. The results of these tests are incomplete but preliminary inspection of weight change data indicate that inconel, as received, showed a significant weight loss, and metallographic examination revealed small voids to a depth of 0.018 in. No other attack was noted. A duplicate of the inconel specimen decarburized in wet hydrogen and similarly tested in the eutectic mixture showed very slight intergranular attack but no measurable weight loss. Photomicrographs of these samples are given in Fig. 2.5. These results are from single samples; future tests are planned to verify them.

LIQUID-METAL CORROSION TESTING: DYNAMIC

Thermal Convection Loops. During the past quarter the metallographic examination of 21 thermal convection loops containing sodium and three containing lead has been completed. Two thermal convection loops operated with lithium and seven operated with lead are being examined. The loops were operated at temperatures up to 1500°F for 1000 hr or until failure occurred. Types 304, 310, 316, 321, and 347 stainless steels, nickel A, inconel, Haynes Alloy 25, and 1010 steel were the materials tested.

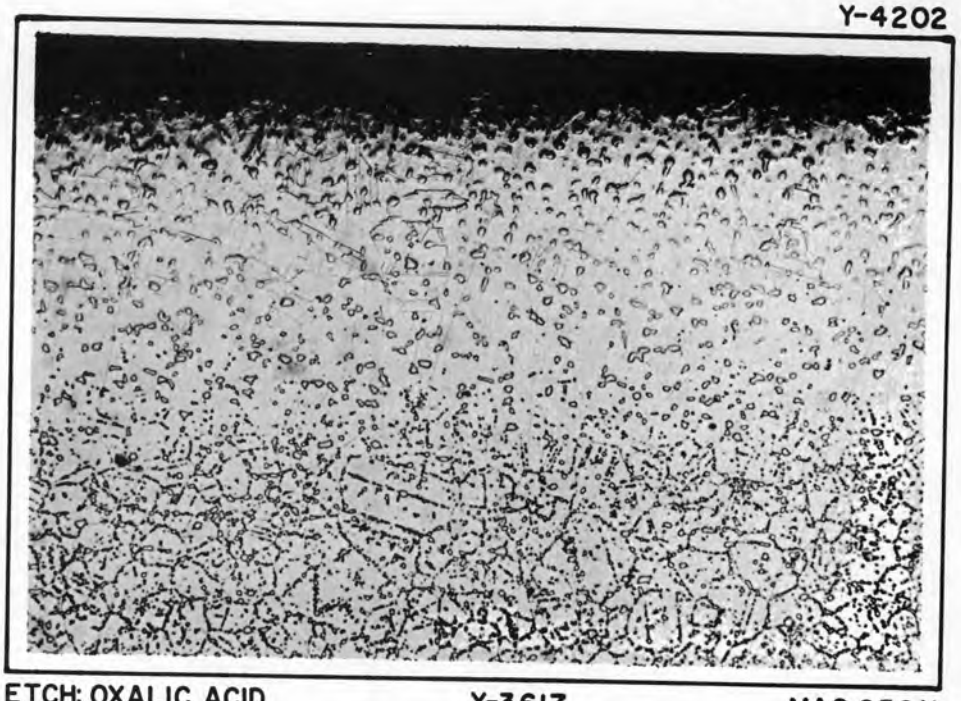

ETCH: OXALIC ACID Y-3617 MAG. 250X

HASTALLOY "B"

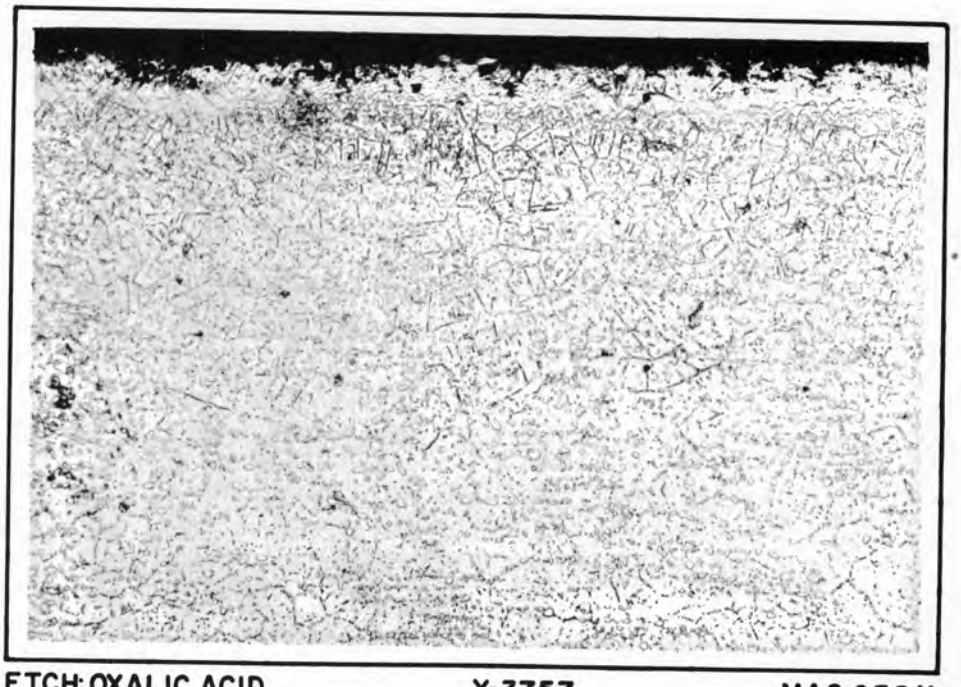

ETCH: OXALIC ACID Y-3757 MAG. 250X

HASTALLOY "C"

HASTALLOYS EXPOSED TO SODIUM FOR 40 HOURS AT 1000° C

FIG. 2.4

NOT CLASSIFIED
Y-4206

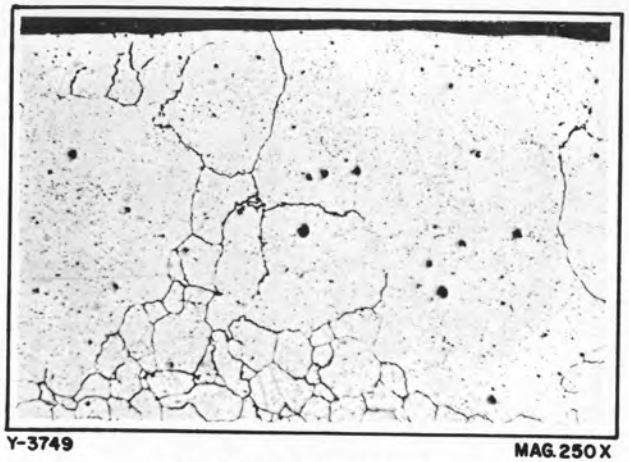

Y-3749 MAG. 250X

DECARBURIZED INCONEL
NOT TESTED

Y-3748 MAG. 250X

DECARBURIZED INCONEL
EXPOSED TO NaF, BeF_2, UF_4 SALT MIXTURE FOR 100 HOURS AT 1000°C
BeF_2 – 10.7%; NaF – 68.0%; UF_4 – 21.3% SALT MIXTURE.

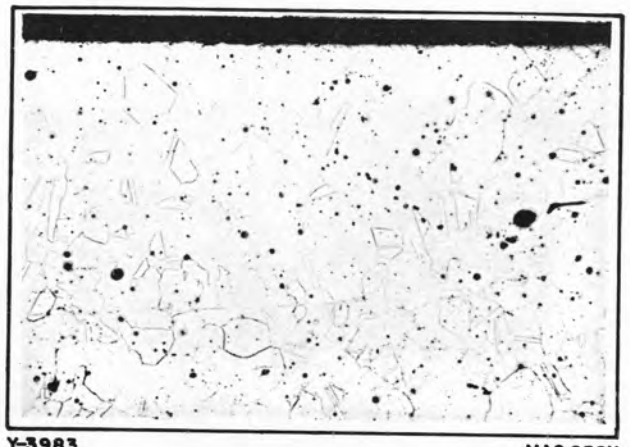

Y-3983 MAG. 250X

INCONEL "AS RECEIVED"
NOT TESTED

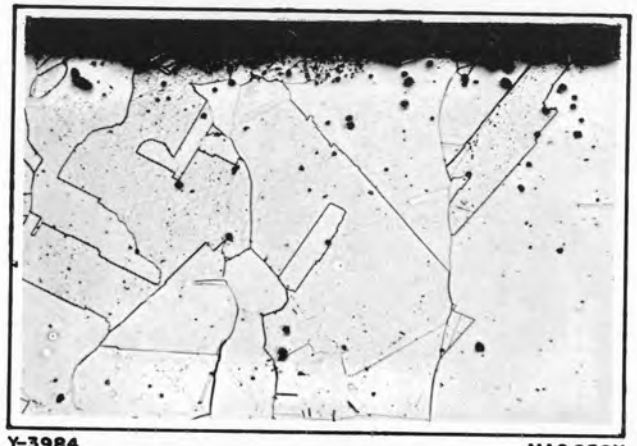

Y-3984 MAG. 250X

INCONEL "AS RECEIVED"
EXPOSED TO NaF, BeF_2, UF_4 SALT MIXTURE FOR 100 HOURS AT 1000°C

COMPARISON OF DECARBURIZED AND "AS RECEIVED" INCONEL

FIG. 2.5

TABLE 2.1

Stainless Steels and Alloys Exposed to Lithium for 400 hr at 1000°C

MATERIAL	DEPTH DISSOLVED (in.)	INTER-GRANULAR PENETRATION (in.)	DEPTH OF DECARBU-RIZATION (in.)	PRECIPITATE OR TRANSFOR-MATION DEPTH (in.)	VOIDS		FILM THICKNESS (in.)	REMARKS	WEIGHT CHANGE (g/sq in.)	ANALYSIS*	
					LOCATION	DEPTH (in.)				X-RAY	BATH (ppm)
304 SS	-0.001	0.010	None	0.003	Grain boundary	0.010	None	Phase transformation uniform along surface except at grain boundaries where it extends inward to 0.010 in.	-0.104	bcc; a_o 2.88	Fe 345 Cr 25 Ni ND Mn 17
304 SS (0.04% C)	-0.003	0.005	None	0.001	Grain boundary	0.005	None	Thin transformed layer extending in at grain boundary to a maximum of 0.005 in.; some voids in this region	-0.423	bcc; a_o 2.87 fcc; a_o 3.57	Fe 604 Cr 870 Ni ND Mn 40
304 SS (0.006% C)	-0.005	0.010	None	0.003	Grain boundary	0.015	None	Same as above except maximum penetration was 0.015 in.	-0.078	No data	No data
316 SS	-0.002	0.015	None	0.015	None		None	Heavy intergranular penetration with phase transformation along attacked grains	-0.163	bcc; a_o 2.87	Fe 204 Cr 36 Ni ND Mo ND
347 SS	0.000	0.010	None	0.010	None		None	Phase transformation along attacked grain boundaries	-0.175	bcc; a_o 2.86	Fe 533 Ni 8 Cb 203 Cr 32
405 SS	0.000	None	None	None		0.004	None	Small voids scattered within grains along exposed surface	-0.054	bcc; a_o 2.86	Fe 315 Cr 25 Al ND
430 SS	0.000	None	None	0.001		0.001	None	Thin, noncontinuous surface constituent containing a few voids	-0.064	bcc; a_o 2.86	Fe 145 Cr 114
446 SS	0.000	None	None	0.008		0.008	None	0.008-in. layer spotted with a fine precipitate and laced with large voids (both in grain boundaries and within grains)	-0.287	bcc; a_o 2.86	Fe 360 Cr 46
446 SS (0.006% C)	0.000	None	None	0.004		0.004	None	Voids near the surface to depth of 0.004 in.; no precipitate seen	-0.108	No data	No data
Inconel	-0.001	0.070	None	None		0.020	None	Very severe intergranular penetration; heavy band of voids extending inward at grain boundaries	-1.848	No data	No data
Inconel X	0.000	0.025	None	None	None		None	Severe intergranular penetration causing surface grains to fall out	-1.262	No data	No data

*bcc = body-centered cubic; fcc = face-centered cubic; ND = not determined; a = lattice constant.

TABLE 2.2

Materials Tested in Lithium 400 hr at 1000°C

MATERIAL	DEPTH DISSOLVED (in.)	INTER-GRANULAR PENETRATION (in.)	DEPTH OF DECARBU-RIZATION (in.)	PRECIPITATE OR TRANSFORMATION DEPTH	VOIDS		FILM THICKNESS (in.)	REMARKS	WEIGHT CHANGE (g/sq in.)	ANALYSIS*	
					LOCATION	DEPTH (in.)				X-RAY	BATH (ppm)
Be	0.000	0.127	None	None	Through-out		None	Complete intergranular penetration; no solution loss; voids both in grain boundaries and within grains	-0.650	Be	Fe 187 Be 298
Ti	-0.001	None	None	None	None		None	Surface rough, indicating solution type attack; weight gain not accounted for	+0.022	Ti	Fe 443 Ti 1056
Co (Mt)**	0.000	0.020	0.020	None		0.020	None	Voids also within grains	-0.779	α Co, Fe, β Co	Fe 86 Co ND
Ni	-0.008	0.023	None	None	None		None	Solution and intergranular penetration; possible breaking off of grains rather than solution	-3.747	Ni	Fe 436 Ni 245
Zr	0.000	None	None	None	None		0.002	Surface compound formation; heavy angular precipitate throughout	+0.020	ZrN	Fe 283 Zr 12
Mo (Mt)**	0.000	None	None	None		0.0005	0.0005	Thin surface deposit, not continuous; appears to be broken off in places; few voids seen under film; no other attack	-0.174	Fe, Mo	Fe 145 Mo ND
Ta	0.000	None	None	None		0.001	0.001	Definite surface film, different structure than base metal	-0.045	TaC	Fe 440 Ta 610
W (Mt)**	-0.005	None	None	None	None		None	Surface rough, appears to have been solution type attack	-1.131	W, Fe, Fe_2W	Fe 383 W 720
Fe	0.000	None	None	0.025		0.025	None	Some voids contain blue-gray particles	-0.004	bcc; a, 2.86	Fe 203
1020 steel	-0.001	None	None	None		0.030	None	Some evidence of blue-gray precipitate in voids before polishing	-0.474	bcc; a, 2.86	Fe 482
1040 steel	+0.003	None	None	None		0.074	None	Voids both in grain boundaries and within grains; distinct odor of acetylene while polishing sample	-0.050	bcc; a, 2.86	Fe 270
Xite	-0.002	0.033	0.033	None	None		None	Cast structure with thick layer of intergranular penetration	-0.811	fcc; a, 3.57	No data
N 155	+0.033	0.064	None	None			None	Heavy intergranular penetration; some voids within grains	-0.554	fcc; a, 3.57	No data

*bcc = body-centered cubic, fcc = face-centered cubic, ND = not determined, a = lattice constant

**(Mt) means mass transfer observed.

Each loop (Figs. 2.6 and 2.7) was constructed of the same material throughout to avoid the presence of a third component in the corrosion test. The loops listed in Tables 2.3 and 2.4 with the exception of Nos. 6, 28, 29, 30, 33, and 34 were fabricated in the ORNL Shops using metal arc welding. These exceptions were fabricated using heliarc welding, loops 6, 28, 29, and 30 at the Philadelphia Pipe Bending Company and loops 33 and 34 in the Y-12 Shops. After fabrication, the loops were cleaned to remove welding scale and surface oxides. The cleaning procedures for the various loops are given on p. 51. Experimental procedures were covered in the previous Metallurgy quarterly report (ORNL-987, p. 48) and will not be repeated here.

With sodium types 347, 321, and 310 stainless steels, inconel, and Haynes Alloy 25 showed very little attack. The iron loop showed some attack. Nickel A and stainless steels 304 and 316 showed some intergranular attack near the weld zones. Owing to the testing variables involved, it has been impossible to determine the exact cause of the intergranular corrosion in the nickel and 304 and 316 stainless steels, but it is not necessarily due to sodium attack.

Loops Operated with Sodium. Eight of the 21 loops that were operated with sodium failed to operate a thousand hours. Four of the eight failures occurred at welds. The welds showed poor penetration of weld metal, and several showed porosity and oxide or slag inclusion. Figure 2.8 shows a typical weld crevice, and Fig. 2.9 shows slag inclusions in the weld metal. The pickling of the loops in uninhibited acid solutions undoubtedly produced some attack of the metal, especially in the weld zones of the unstabilized stainless steels, making the metallographic examination of these loops difficult to interpret. The attack which occurred during pickling cannot be differentiated from the attack which occurred during operation with sodium, and the data should be interpreted with caution.

The 1010 steel loop No. 8 failed by external oxidation in the hot zone. In the top cup the wall thickness was reduced 20 mils at the liquid-metal level. The hot zone region had a bright metallic surface, indicating the reduction of any surface oxide films and the absence of any corrosion products. The bottom cup contained a considerable amount of a dark residue that analyzed 2.7% carbon and over 95% iron. Spectrographic analyses of sodium from the bottom cup showed appreciable amounts of iron present. The oxygen content of the sodium increased during operation, indicating the reduction of surface oxide on the metal. The attack was heavier in the hot than in the cold zone, and was not intergranular in nature.

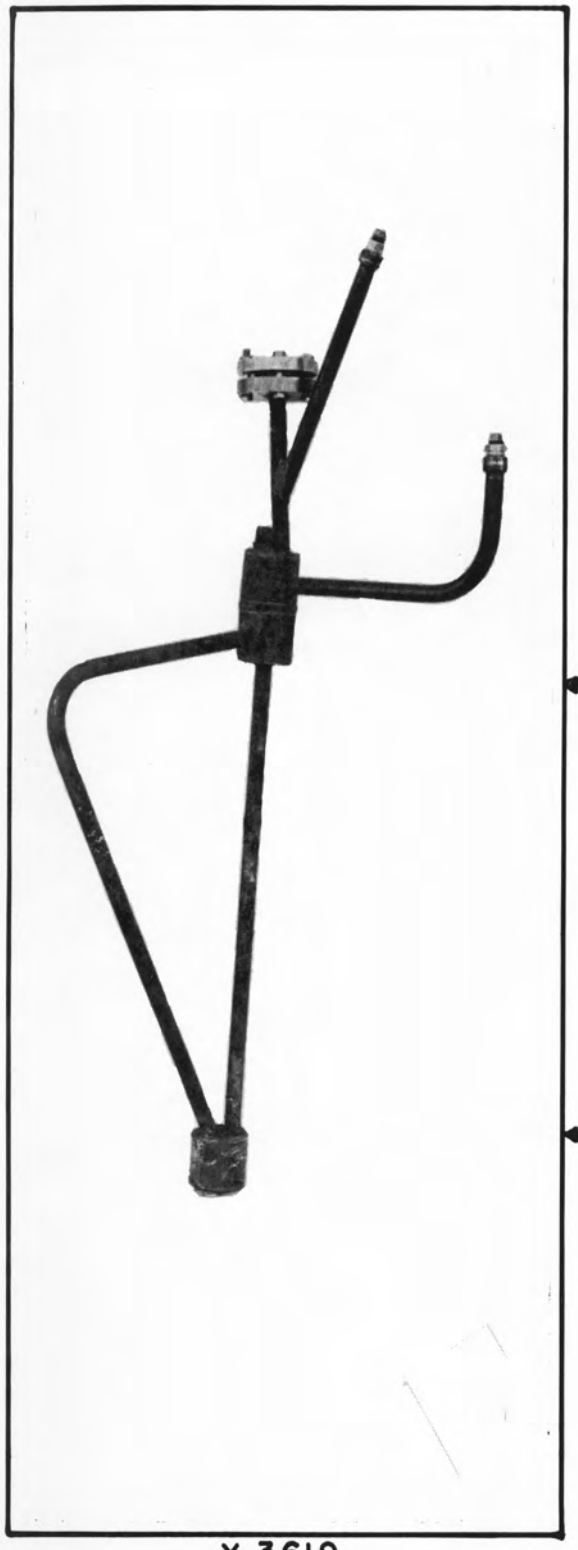

Y-3619

OLD DESIGN

FIG. 2.6

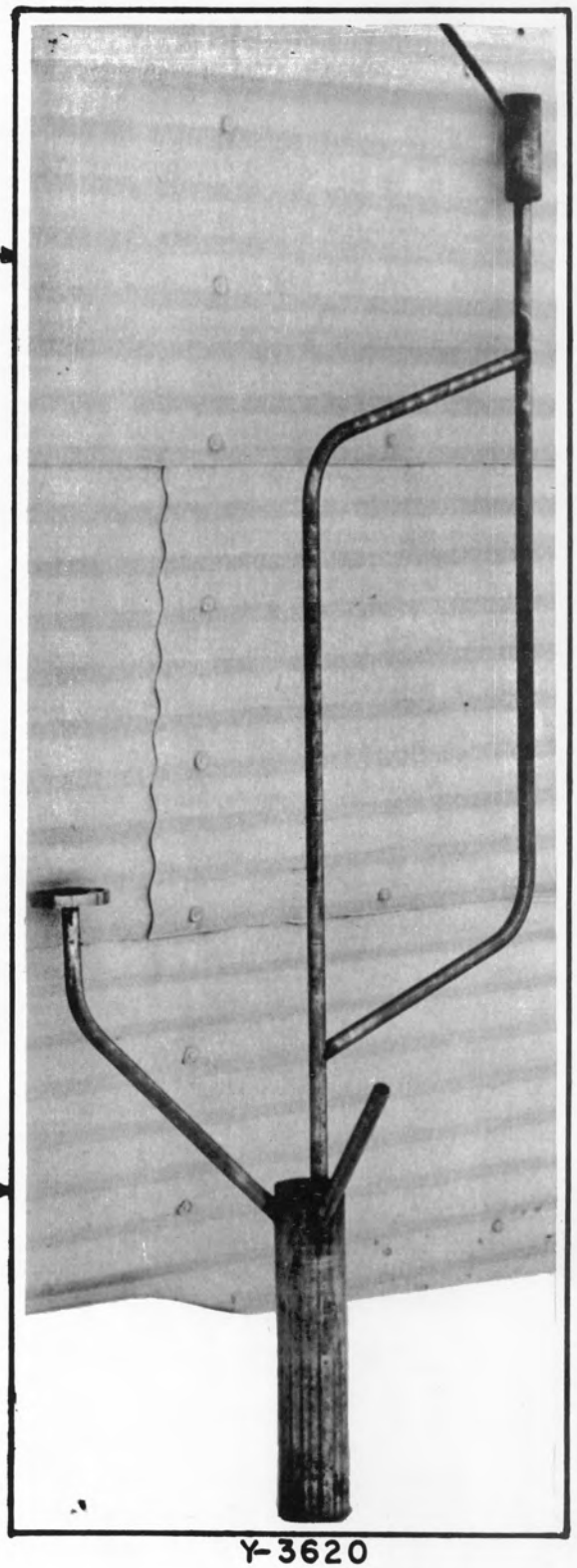

Y-3620

NEW DESIGN

FIG. 2.7

THERMAL CONVECTION LOOP

NOT CLASSIFIED
Y-3743

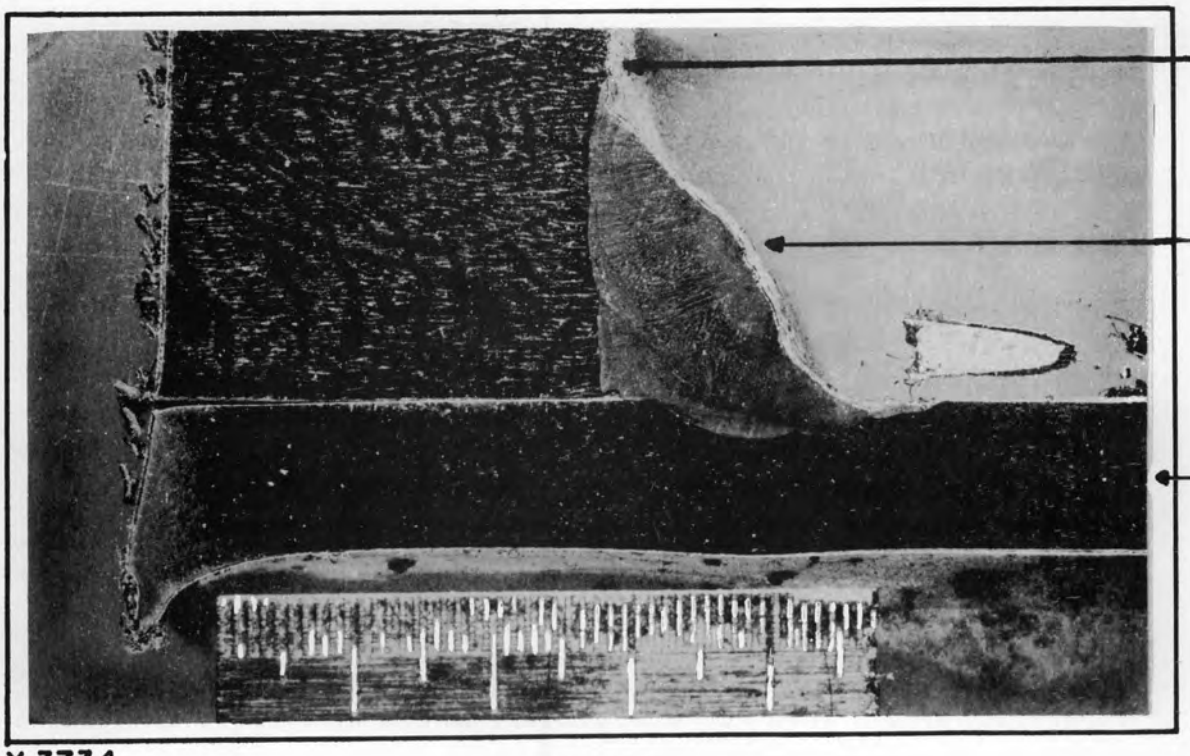

Y-3734

FIG. 2.8

WELD CREVICE IN 316 STAINLESS STEEL LOOP (NO. 2)

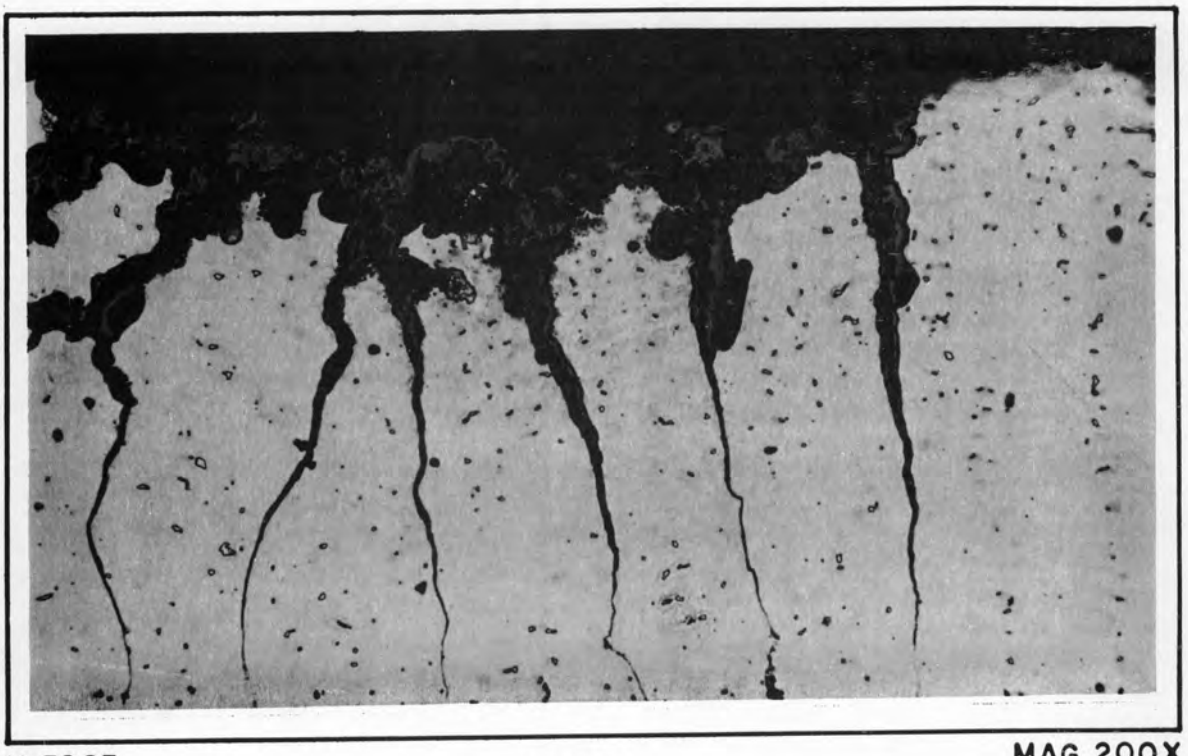

Y-3263

MAG. 200X

FIG. 2.9

OXIDE INCLUSIONS IN WELD METAL OF 304 STAINLESS STEEL LOOP (NO. 5)

TABLE 2.3

Corrosion and Operation Data of Thermal Convection Loops Containing Sodium

LOOP NO.	LOOP MATERIAL	LENGTH OF TEST (hr)	HOT-ZONE TEMPERATURE (°F)	COLD-ZONE TEMPERATURE (°F)	REMARKS	TIME OF SAMPLING	LOCATION OF SAMPLE	OXYGEN ANALYSES (%)		SPECTROGRAPHIC ANALYSES OF SODIUM FOR CORROSION PRODUCTS (ppm)						METALLOGRAPHIC EXAMINATION
								UPPER BULB	LOWER BULB	Fe	Cr	Ni	Mo	Mn	MISCEL-LANEOUS	
1	316 SS	1100	1350	1130		Initial	Top	0.092	0.082							Appreciable amounts of sigma formed in the two loops operated at 1500°F, more in hot zones than in cold; all four loops showed heavy intergranular attack in bottom cups near welds; most specimens had a slight irregular edge, indicating some attack
						Final	Top	0.028	0.014	30	<30	<130	<75	<30		
						Final	Bottom			90	<15	<70	<15	<15		
2	316 SS	978	1350	1110	Gas line failure	Initial	Top	0.056	0.013							
						Final	Top			1130	50	<250	<50	<50		
						Final	Bottom			15	<5	<20	<5	<5		
3	316 SS	1000	1500	1345		Initial	Top	0.067	0.087							
						Final	Top	0.021	0.012	210	<105	<470	<260	<105		
						Final	Bottom			1200	<40	<200	<40	<40		
4	316 SS	625	1500	1165	Hot-zone failure	Initial	Top	0.086								
						Final	Top	0.031	0.020	120	<25	<120	<25	<25		
						Final	Bottom			20	<5	<20	<5	<5		
5	304 SS	349	1500	1270	Weld failure	Initial	Top	0.032								Considerable intergranular attack of weld metal, heaviest in the cold-zone welds; most specimens had a slight irregular edge, indicating some attack
						Final	Bottom			1680	580	270	<10			
16	304 SS	988	1350	1185		Initial	Top	0.037	0.051							
						Final	Top	0.011	0.016	<75	<35	<180	<95	<35		
						Final	Bottom			20	10	<50	<10	<10		
17	304 SS	1000	1350	1220		Initial	Top	0.052	0.016							
						Final	Top	0.015	0.011	30	<30	<140	<30	<30		
						Final	Bottom			50	<5	<20	<5	<5		
7	347 SS	1000	1500	1290		Initial	Top	0.020	0.013							No intergranular attack on samples and very little evidence of any type of corrosion
						Final	Top	0.008	0.018	<150	<70	<370	<180	<70		
						Final	Bottom			20	<5	<25	<15	<5		
14	347 SS	1000	1350	1110		Initial	Top	0.037	0.090							
						Final	Top	0.009	0.027	<70	<35	<170	<85	<35		
						Final	Bottom			30	<5	<25	5	<5		
15	347 SS	1000	1350	1175		Initial	Top	0.025	0.019							
						Final	Top	0.045	0.023	<45	<25	<110	<55	<25		
						Final	Bottom			30	<5	<30	<5	<5		
30	310 SS	1000	1350	1185		Initial	Top	0.015	0.008							Metallographic examination showed evidence of sigma formation in hot zone; very little attack evident on samples
						Final	Top	0.022	0.022	70	100	10	<5	15		
						Final	Bottom			<10	5	<20	<5	<5		
33	321 SS	754	1500	530-850	Failed middle of top section	Final	Bottom	0.012	0.016	20	5	<25	<5	<5	<10 Ti	Metallographic examination showed heavy internal oxidation near weld zones of loop 34, which was thought to have occurred during welding; pipe samples from No. 34 and all samples from No. 33 showed only slight attack
						Final	Bottom	0.021	0.012							
34	321 SS	457	1500	1050	Unable to maintain circulation	Final	Bottom	0.079	0.074	40	50	<35	<5	35	30 Ti	
6	Haynes Alloy No. 25	1000	1500	1290		Final	Top			70	95	500	<25		270 Co <230 W	No evidence of corrosion in any samples
						Final	Bottom			20	10	<40	<10		<40 Co <80 W	

TABLE 2.3 (Cont'd)

LOOP NO	LOOP MATERIAL	LENGTH OF TEST (hr)	HOT-ZONE TEMPERATURE (°F)	COLD-ZONE TEMPERATURE (°F)	REMARKS	TIME OF SAMPLING	LOCATION OF SAMPLE	OXYGEN ANALYSES (%)		SPECTROGRAPHIC ANALYSES OF SODIUM FOR CORROSION PRODUCTS (ppm)						METALLOGRAPHIC EXAMINATION
								UPPER BULB	LOWER BULB	Fe	Cr	Ni	Mo	Mn	MISCELLANEOUS	
8	1010 steel	593	1200	840	Loop failed by external oxidation	Initial Final Final	Top Top Bottom	0.021	0.017 0.043	110 11200	60 610	280 55	60 30	60 160		When loop was opened considerable attack was noted in top cup and bottom cup contained a considerable amount of a dark metallic residue that analyzed 2.7% carbon and over 95% iron; attack was fairly uniform, as little evidence of attack could be seen in metallographic samples
10	1010 steel	25	1200	1000	Weld failure in bottom cup	Initial Final	Top Top	0.047 0.039	0.025 0.025							Metallographic examination showed voids and poor bonding between parent and weld metal in bottom cup
13	Nickel A	223	1500	1020	Weld failure in bottom cup	Initial Final Final	Top Top Bottom	0.027	0.026			8500 3300				All samples showed light attack, not intergranular, which was especially heavy near weld failure
11	Nickel A	13	1500	1310	Weld failure in bottom cup	Initial Final Final	Top Top Bottom	0.033	0.063			4100 245				Metallographic examination showed poor bonding between parent and weld metal in bottom cup
12	Nickel A	1000	1500	1250		Initial Final Final	Top Top Bottom	0.046 0.024	0.025 0.019	15 10	<5 5	650 <30				Metallographic examination showed little attack on pipe samples, but heavy intergranular attack of pipe and plate material occurred adjacent to weld zones
9	Nickel A	0			Failed in cold zone											Loop failed where two pieces of ½-in. pipe had been butt-welded together; this was from a flaw in the material when received
29	Inconel	1000	1350	1200		Initial Final Final	Top Top Bottom	0.023	0.011		<5 <5	<10 <15			10 Cu <5 Cu	Pipe samples showed slight amount of intergranular attack

TABLE 2.4

Corrosion and Operation Data of Thermal Convection Loops Containing Lead

LOOP NO.	LOOP MATERIAL	LENGTH OF TEST (hr)	HOT-ZONE TEMPERATURE (°F)	COLD-ZONE TEMPERATURE (°F)	REMARKS	LOCATION OF SAMPLE	CHEMICAL ANALYSES OF LEAD FOR CORROSION PRODUCTS (%)					METALLOGRAPHIC EXAMINATION
							Fe	Ni	Cr	Mo	O_2	
26	316 SS	138	1500	1300	Loop plugged internally during operation	Cold zone lead	0.03	0.03	0.001	0.004	0.0046	Hot-zone samples showed considerably more attack than cold-zone samples, the surfaces of the samples showing pronounced irregularities; cold-zone sections of loop were blocked with lead plug in which was a network of dendritic crystals of the loop material
						Cold zone lead	4.6	0.6	1.39	0.005	0.048	
						Hot zone lead	0.004	0.03	0.001	0.004		
27	316 SS	0			Loop plugged during filling							Loop was heated too long during filling and plugged in the cold zones; metallographic examination of the plugged material showed it to consist of dendritic crystals of the loop material in a lead matrix
28	446 SS	62	1500	1300	Loop plugged internally during operation	Cold zone lead	0.67		0.001		0.002	Hot-zone samples showed very heavy attack; wall thickness of hot zone was 12 mils less than that of cold zone; hot zone showed a spongy type of attack, the spongy layer being about 3 mils thick; as in loop 26, cold zone was blocked with a lead plug containing dendritic crystals of the loop material
						Cold zone lead	7.8		2.92		0.047	
						Hot zone lead	0.08		0.001		0.0046	
						Hot zone lead	5.1		4.64		0.048	

Metallographic samples taken from the Haynes Alloy 25 loop, No. 6, showed no evidence of attack. Spectrographic analysis of the sodium from the loop showed the presence of small amounts of iron, chromium, nickel, and cobalt.

Metallographic samples from nickel loop No. 13 showed only light attack, while metallographic samples from nickel loop No. 12 showed heavy intergranular attack in the parent metal near the weld zones. This intergranular attack (Fig. 2.10) was not present in the pipe samples away from the weld zone (Fig. 2.11). It is believed that the presence of sulfur-containing lubricants during welding caused the formation of an intergranular layer of nickel sulfide which was removed during either pickling or operation with sodium. Spectrographic analyses of the sodium from both loops showed appreciable amounts of nickel present. Mass transfer of nickel occurred in the cold zone of nickel loop No. 12 (Figs. 2.12 and 2.13). The mass-transferred material was in the form of spongy dendritic crystals adhering loosely to the walls of the bottom cup. Spectrographic analysis showed the material to be nickel with traces of chromium, iron, and manganese. X-ray diffraction analyses identified the material as nickel (face-centered cubic structure with a lattice parameter 3.512 A).

The oxygen content of the sodium decreased during the operation of all the 300 series stainless steels, indicating some reaction with the stainless steel. Types 347 and 321 showed the best resistance to attack of any of the 300 series. There was no evidence of attack in the metallographic specimens and the spectrographic analyses of the sodium showed only small amounts of corrosion products present. The weld zones of one of the 321 stainless steel loops showed heavy oxidation, indicating no inert protective gas had been used during welding. The metallographic samples from the 304 and 316 stainless steels showed more general attack than samples of type 347, and the cold-zone weld samples of the 316 stainless steel loops showed localized areas of very heavy intergranular attack of the parent metal (Fig. 2.14). The weld metal of several of the type 304 stainless steel loops showed intergranular attack (Fig. 2.15). The unstabilized metal was probably made susceptible to intergranular attack during welding. This intergranular attack could have occurred during pickling or during operation with sodium. During pickling, the loops were immersed in the pickling solution, and it is difficult to understand why the weld zones in the hot section should not be subject to the same attack as those in the cold zone. During operation with sodium, it is possible that the

Y-3469 MAG. 100X

FIG. 2.10

INTERGRANULAR ATTACK NEAR THE WELD OF NICKEL LOOP (NO. 12)

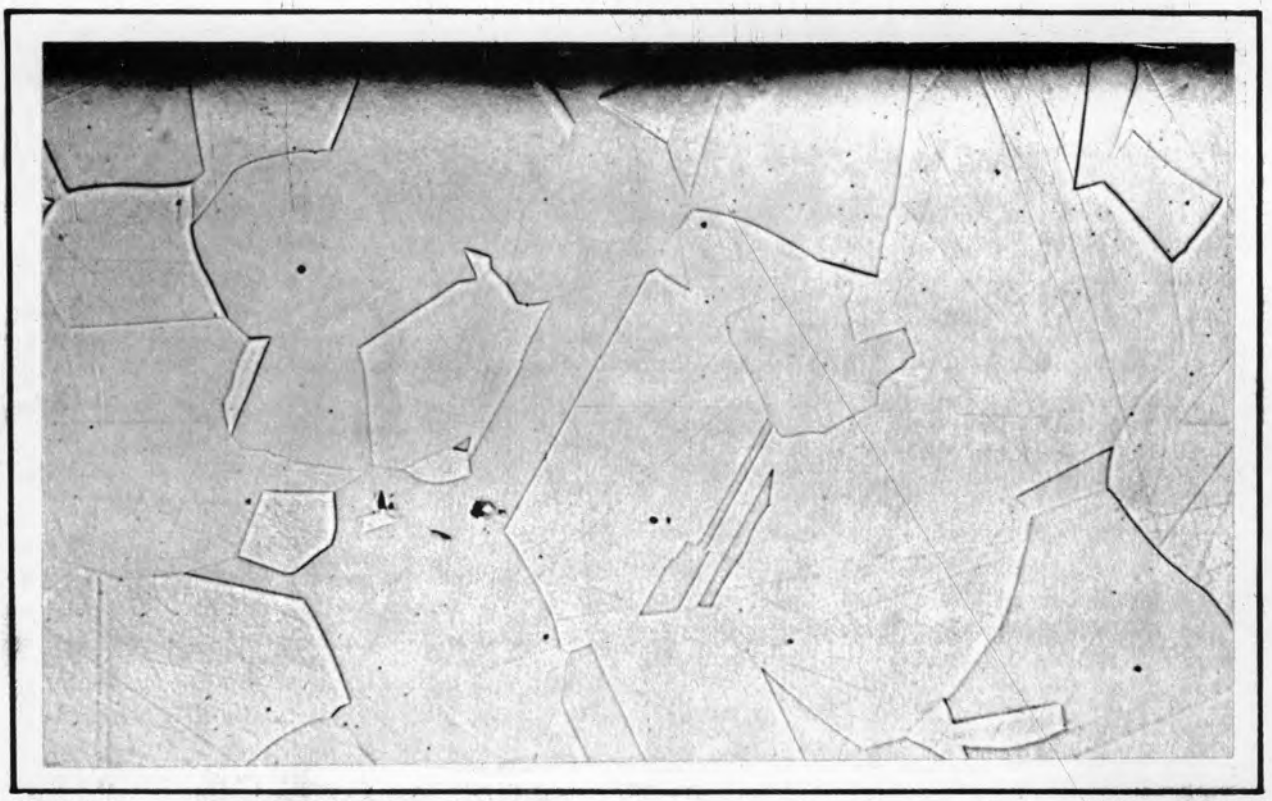

Y-3471 MAG. 200X

FIG. 2.11

PIPE SAMPLE FROM NICKEL LOOP (NO. 12) NOT ADJACENT TO WELD ZONE

NOT CLASSIFIED
Y-3739

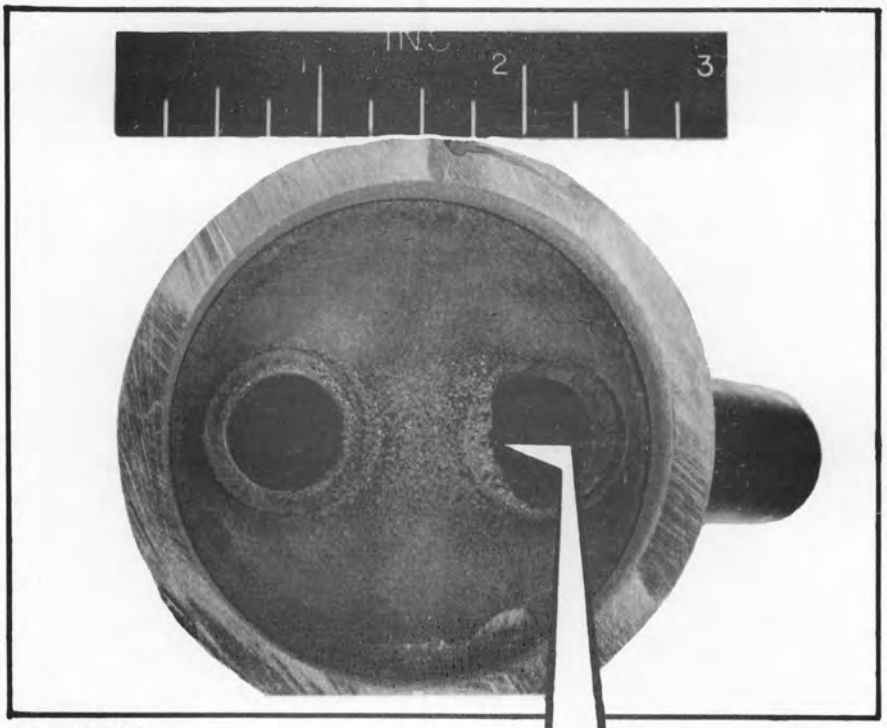

Y-3226

FIG.2.12

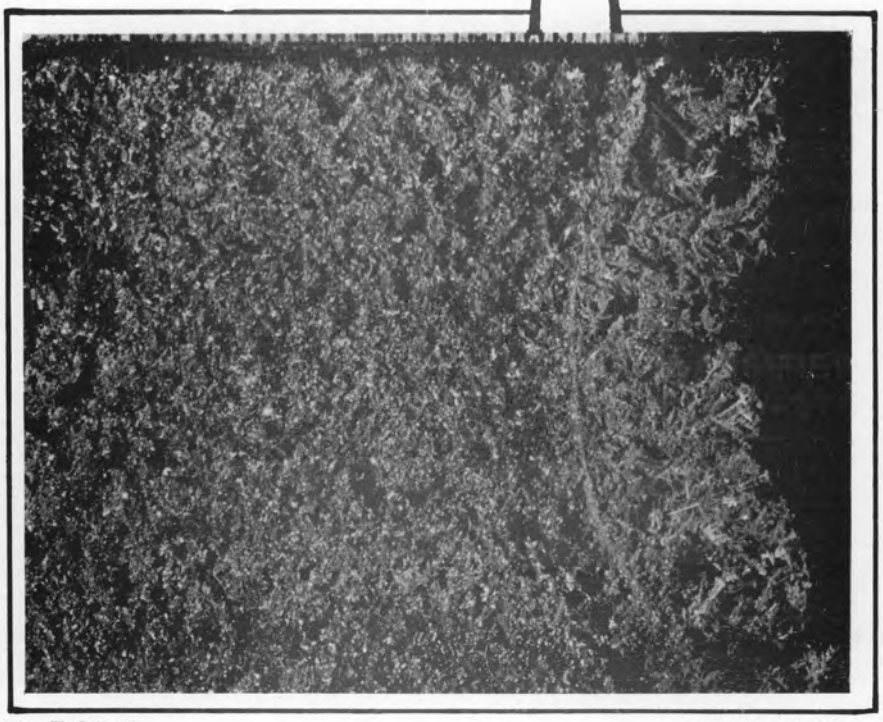

Y-3233 MAG. 8 X

FIG.2.13
MASS TRANSFER MATERIAL IN COLD ZONE OF NICKEL LOOP (NO.12)

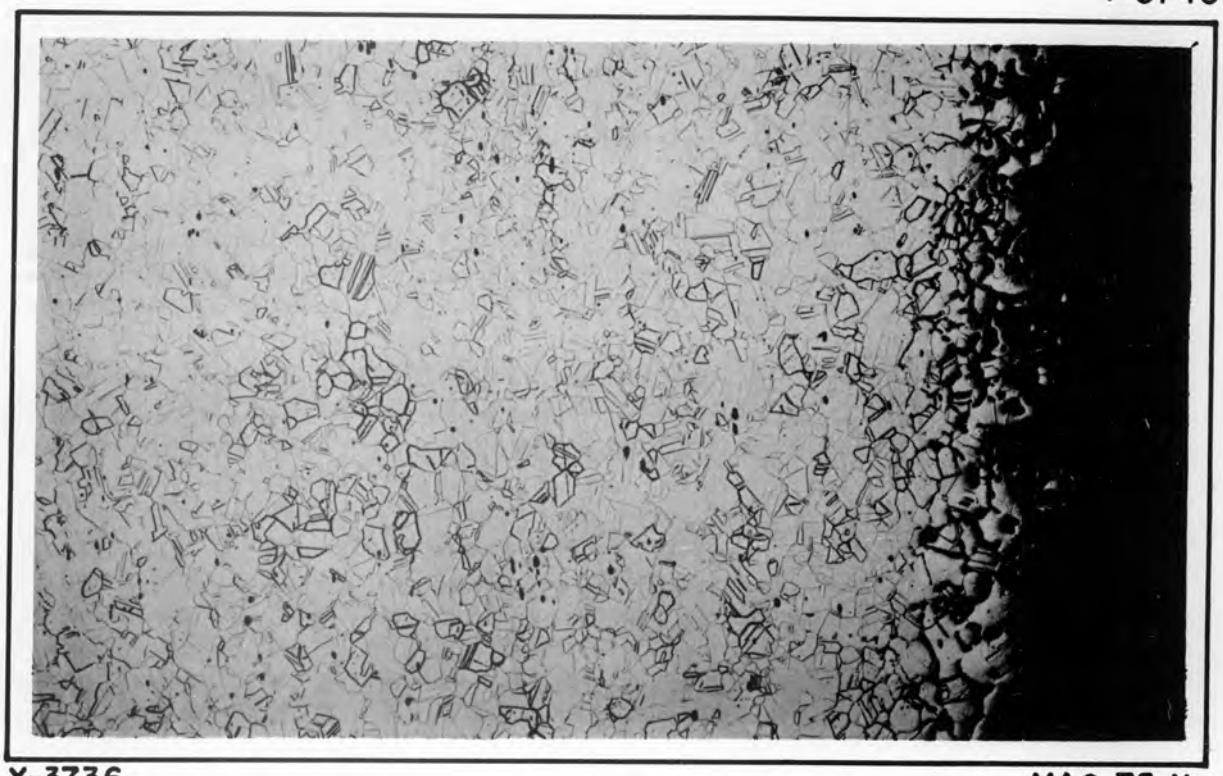

Y-3736 MAG. 75 X

FIG. 2.14
INTERGRANULAR ATTACK NEAR THE WELD IN 316 STAINLESS STEEL LOOP (NO. 1)

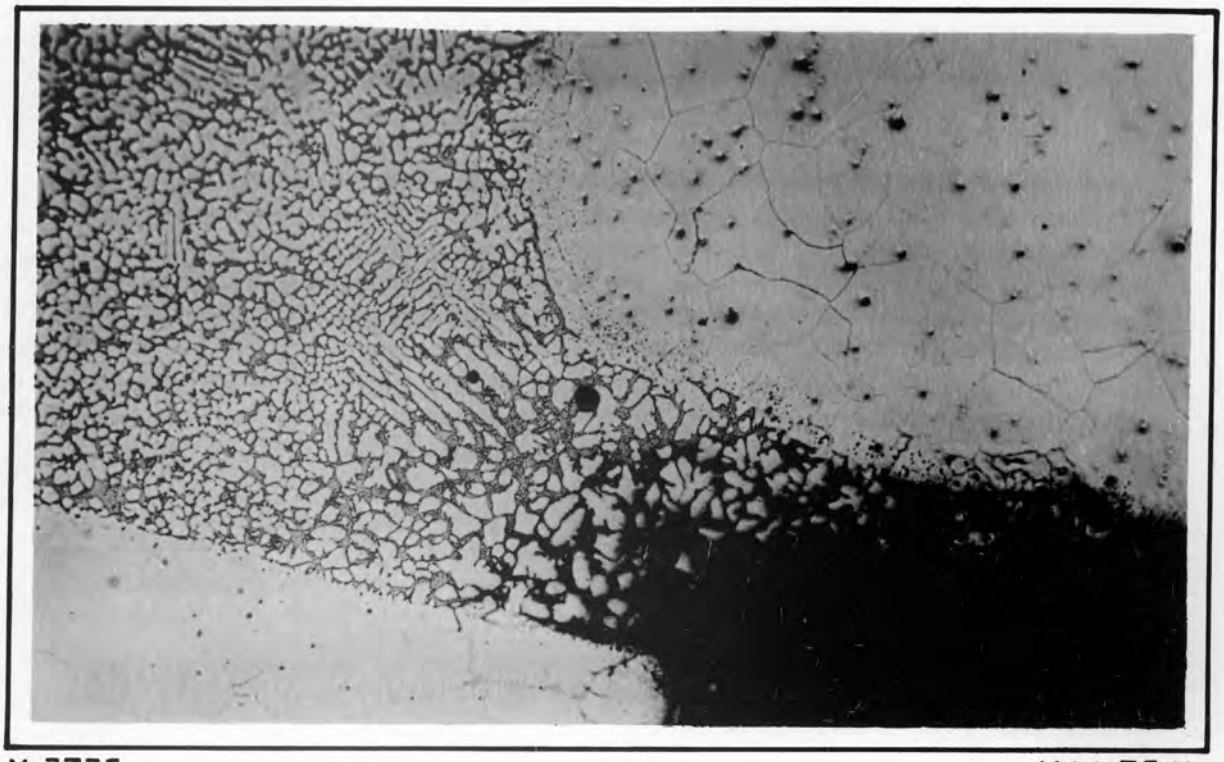

Y-3735 MAG. 75 X

FIG. 2.15
INTERGRANULAR ATTACK NEAR THE WELD IN 316 STAINLESS STEEL LOOP (NO. 16)

gravity segregation of sodium oxide in the bottom cup might have locally increased the attack and been the cause of this intergranular corrosion. It is of interest to note that loop No. 30 (310 stainless steel), which was not pickled, did not show the intergranular attack in the weld zone.

Metallographic samples from the inconel loop No. 29 showed some intergranular attack in the pipe section (Fig. 2.16), but only light general attack in the weld zone region.

When a loop failed during operation and sodium came into contact with the external surface of the loop, very heavy attack (Fig. 2.17) of the external surface took place. This attack was noted on loops 5, 9, 10, 11, and 13. The attack is believed to have been caused by the large amounts of sodium oxide formed when the sodium came into contact with the air.

Loops Operated with Lead. All three lead-containing loops (Table 2.4) failed because of internal obstructions (plugging). The plugs, which occurred in the cold zone, consisted of dendritic-like crystals of a high-melting metal, and probably represent transfer due to temperature gradients in the loop. Chemical analyses of the plugs showed them to consist essentially of iron, chromium, and nickel in the 316 stainless steel loop, and of iron and chromium in the 446 stainless steel loop. The hot-zone samples showed considerably more attack than the cold-zone samples.

Current Experiments. In conjunction with the Aircraft Reactor Experiment the emphasis in the dynamic corrosion program is now being placed on the testing of inconel and the 300 series stainless steels in sodium, and all dynamic corrosion tests with lithium and lead have been temporarily discontinued. At present the following sodium-containing loops are being operated by the ANP Experimental Engineering Group at a maximum temperature of 1500°F for 1000 hr or until failure occurs. Additional thermal convection loops are being fabricated for operation with sodium.

LOOP MATERIAL	REMARKS
304 stainless steel	Loop contains beryllium samples
304 stainless steel	Loop contains molybdenum samples
309 stainless steel	
316 stainless steel	1% Na_2O_2 by weight added to loop
Inconel	Loop contains beryllium samples

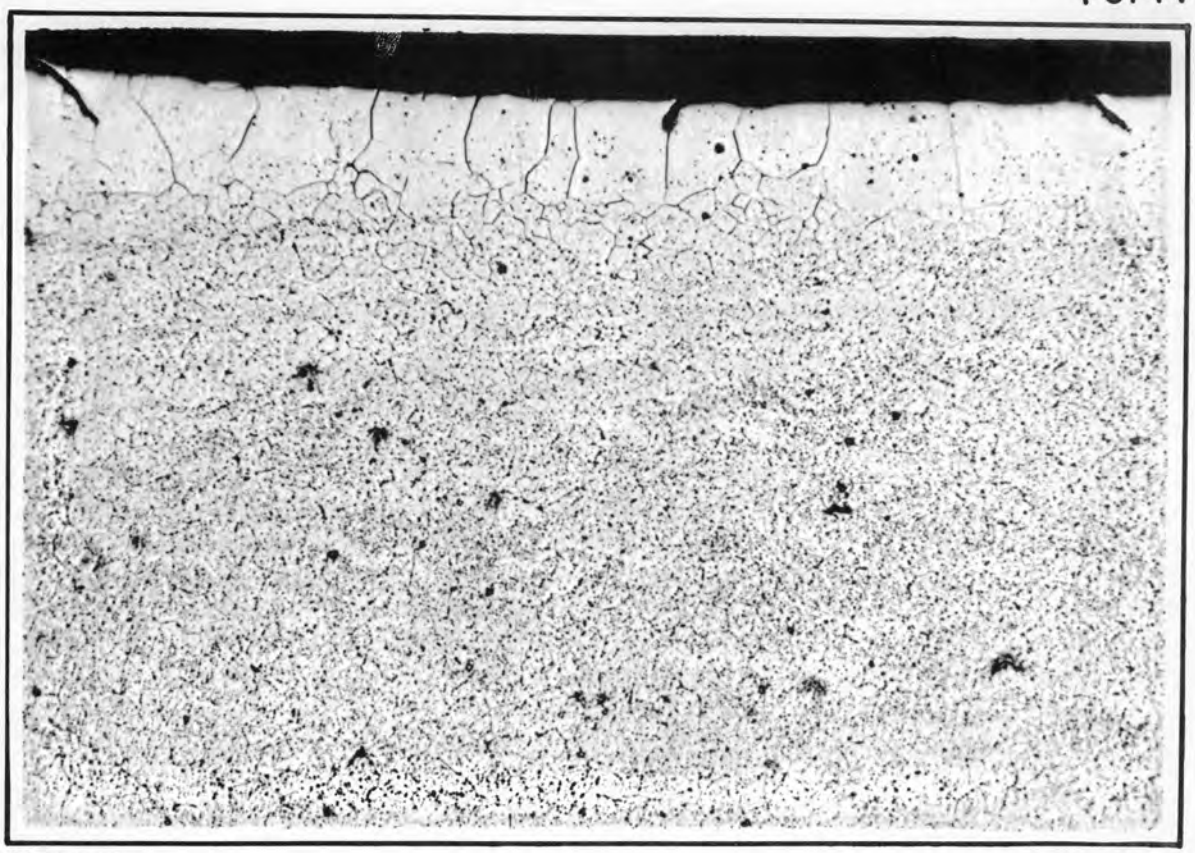

Y-3472 MAG. 200X

FIG. 2.16
INTERGRANULAR ATTACK IN INCONEL LOOP (NO. 29)

Y-3501

FIG. 2.17
ATTACK ON EXTERNAL SURFACE OF NICKEL LOOP (NO. 11) CAUSED BY SODIUM AND SODIUM OXIDE AFTER FAILURE OF LOOP.

Inconel	Loop contains molybdenum samples
Inconel	1% Na_2O_2 by weight added to loop
410 stainless steel	
430 stainless steel	
430 stainless steel	1% Na_2O_2 by weight added to loop
Inconel X	

Cleaning Procedures. *Degreasing.* The degreasing procedure used for all materials was to immerse the loop in a 10% (by weight) trisodium phosphate solution at 200°F for 15 min followed by two warm water rinses.

Pickling Procedure for 300 Series Stainless Steel Loops. The loop was immersed in acid solution (10% sulfuric acid, 10% hydrochloric, 80% water by volume) at 180°F for 1 hr, followed by warm and cold water rinses. It was then immersed in another acid solution (10% nitric acid, 2.5% hydrofluoric acid, and 87% water by volume) at 170°F for 30 min, followed by hot and cold water rinses. This procedure was used on loops 1, 2, 3, 4, 5, 7, 14, 15, 16, and 17.

Pickling Procedure for Nickel Base Loops. The loop was immersed in an acid solution (2 gal of water, 1 gal of hydrochloric acid, ½ lb of cupric chloride) at 180°F for 30 min, followed by a dip in a 50% solution of hydrochloric acid, and then by warm and cold rinses. This procedure was used on loops 9, 11, 12, and 13.

Pickling Procedure for Low-Carbon-Steel Loops. The loop was immersed in an acid solution (8 fluid oz. of hydrochloric acid, 10 fluid oz. of sulfuric acid, 1 gal of water) at 180°F for 20 min, followed by a rinse in 50% hydrochloric acid and cold and hot water rinses. This procedure was used on loops 8 and 10.

Pickling Procedure for Cobalt-Base Alloy Loops. The same pickling procedure was used as for the 300 series stainless steels, followed by a rinse with 50% hydrochloric acid solution and rinses in hot and cold water. This procedure was used on loop 6.

The pickling procedures were used only on loops 1 through 17, inclusive. At present, material is pickled only where it is necessary to remove scale for welding. All pickling is done in inhibited pickling solutions, and samples of the material are taken before and after pickling to determine if any attack of the parent metal has occurred.

Water Removal Procedure Used on All Loops. The loop was rinsed twice with methyl alcohol and once with ether. The loop was then vacuum pumped down to an absolute pressure of 20 μ Hg or less.

Forced Circulation Loops. The ANP Experimental Engineering Group is currently operating a forced convection loop constructed of type 316 stainless steel. Two type 347 stainless steel loops and two inconel loops are being fabricated for use with sodium, and several more are in the design stage. Test sections for determining stress-rupture and stress-corrosion data have been completed and will be used initially on specially built thermal convection loops to obtain stress-rupture data for the Aircraft Reactor Experiment.

POWDER METALLURGY

Fuel Element Fabrication. Work on the fabrication of a solid type fuel element for a high-temperature reactor is progressing. The three methods of fabrication of a fuel plate that have been actively pursued during this quarter are:

1. Filling the holes in a perforated or mechanically deformed metal plate with UO_2 and cladding by solid-phase bonding.
2. Sintering and bonding a loose powder to a back-up plate.
3. Pressing a powder compact and cladding with a hot-rolling technique similar to that used in producing MTR plates.

Mechanically Formed Matrix. Work continued during this quarter on mechanical punching and embossing methods for fabrication of fuel-supporting matrices. A macrograph of the Hendrick Manufacturing Company's 0.020-in.-diameter punched hole design was presented in the last quarterly report (ORNL-987). An improvement in both precision and open area of 0.007-in. hard brass sheet is shown in Fig. 2.18. This screen was supplied by the Norton Company; the holes comprise 33% of the area.

The X-10 Research Shops expressed confidence in being able to produce similar-sized openings but with overall open area of about 65%. Accordingly, a simple die and semiautomatic punch press equipment is being assembled to produce 1-in.-wide molybdenum strip, 0.005 in. thick, having a close-packed

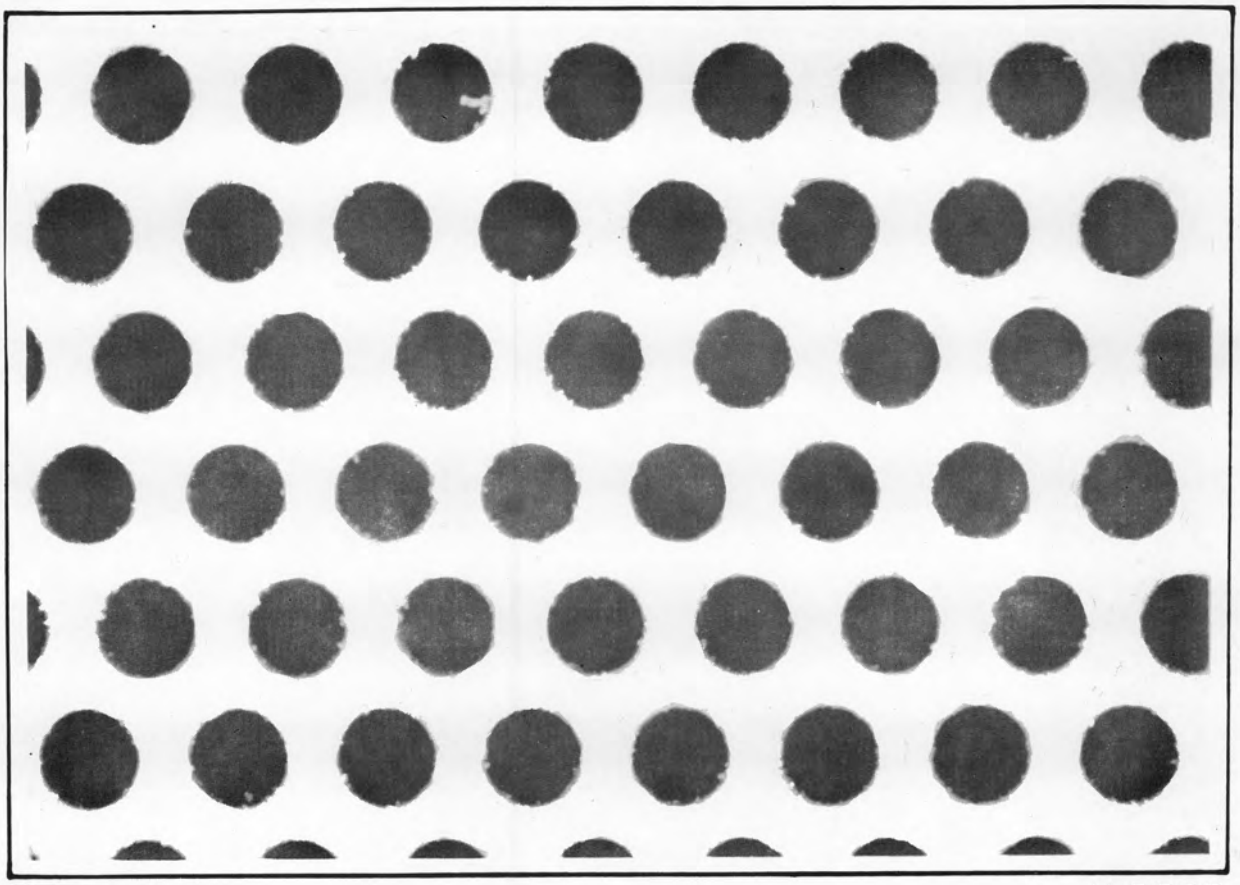

MAG. 28X

Y-3392

SHEET– 0.007 in. THICK
HOLES– 0.020 in. DIAMETER
33% OPEN AREA

PERFORATIONS IN HARD BRASS SHEET

FIG. 2.18

0.020-in.-diameter hole arrangement on 0.025-in. centers. Preliminary hand-punch experiments have demonstrated the feasibility of supporting-web sections as small as 0.002 to 0.004 in.

Another approach to the continuous-sheet matrix problem concerns the use of embossed metal foil. A preliminary test strip of 0.002-in. steel foil was prepared by the Royal Lace Paper Works, Inc. They successfully employed a "till" design roller die which imparted a 0.010-in. raised pattern of circular dimples, running about 700 per square inch. A rolled diamond pattern of sharp ridges is also being considered, as this design can readily be produced on the lace paper machines.

Solid-phase welding tests were conducted at the Micro Metallic Corporation. Twelve 1½- by 2-in. packets comprising sandwiched sheet specimens of various stainless steels, molybdenum, electroformed nickel screening, stainless steel wire screening, and sheets electroplated with flash coats of nickel, iron, and chromium were tried. A dead-weight pressure of approximately 1½ psi was used, the reported temperature being about 1325°C for about 2 hr. Unfortunately, this production furnace is not operated under known conditions within the muffle. From an examination of the run it is apparent that certain specimens were highly overheated; in several locations melting had occurred. Metallographic studies are currently being performed on all specimens. In some cases extensive diffusion and bonding is evident; other interfacial areas are shown to be unbonded or fractured, owing perhaps to brittle phases being formed. There are indications that chromium-plated molybdenum may self-bond efficiently under the conditions used.

Sintering and Bonding a Loose Powder. Work on achieving a bond by sintering loose powders to a back-up plate has been continued, using equipment at the Micro Metallic Corporation in New York. In Table 2.5 are given the results, which are based only upon a visual examination of a bend in the plate and so must be regarded as preliminary. The metallographic examinations have not been completed. The table is divided into two parts; in the top half the plates were sintered as assembled, while with those in the lower half a dead load of 0.5 psi was applied to increase the contact. These data show that the surface preparation of the base plate is not as important as expected and that the substitution of iron or nickel powder for the stainless steel powder looks doubtful.

TABLE 2.5

Loose Powder Sintering and Bonding

POWDER LAYER	PLATE	COMMENTS
	AS ASSEMBLED	
20% UO_2* + G-316 stainless steel	Degreased 316 stainless steel	Well bonded
G-316 stainless steel	Electropolished 316 stainless steel	Well bonded
G-316 stainless steel	Slightly roughened 316 stainless steel	Well bonded
G-316 stainless steel	Heavily roughened 316 stainless steel	Well bonded
10-μ carbonyl Fe	Degreased 316 stainless steel	Poor bonding
325 mesh hydrogen-reduced Fe	Degreased 316 stainless steel	No bonding
10-μ carbonyl Ni	Degreased 316 stainless steel	No bonding
10-μ carbonyl Fe	Fe-plated 316 stainless steel	Poor bonding
10-μ carbonyl Fe	Ni-plated 316 stainless steel	Fair bonding
10-μ carbonyl Ni	Ni plated 316 stainless steel	No bonding
G-316 stainless steel	Ni-plated 316 stainless steel	Poor bonding
	WITH 0.5 psi DEAD LOAD	
20% UO_2* + G-316 stainless steel	Degreased 316 stainless steel	Well bonded
Carbonyl Fe	Degreased 316 stainless steel	Poor bonding
G-316 stainless steel	Ni-plated molybdenum	Fair bonding
Mo	Ni-plated molybdenum	Fair bonding
Cr	Ni-plated molybdenum	Poor bonding
40% UO_2* + G-316 stainless steel	Degreased 316 stainless steel	Slight bonding
Carbonyl Fe	Degreased 316 stainless steel	Poor bonding

*By volume.

Since the furnace at the Micro Metallic Corporation is primarily a production furnace it is not possible to control the time, temperature, and atmosphere variables within the limits necessary for our work. Further work on this problem will be left until we can use our own equipment.

Hot-Rolled Clad Fuel Plate. With this procedure for producing a fuel plate, a core of UO_2 and a matrix of some metallic powder is first pressed. This core is clad by hot rolling, using a technique similar to that used for producing MTR fuel plates.

In the last quarterly report it was pointed out that when stainless steel powders were used as the matrix material there was a tendency for the UO_2 particles to agglomerate and to form stringers. Figure 2.19 shows that this is a particle size phenomenon and may be eliminated by using very fine particles. Figure 2.20 demonstrates that this effect is also present with iron powders but not to such a degree. The sections with the fine powders show that with 50% UO_2 a continuous metallic network and good bonding still may be obtained.

A series of plates was made in which inconel was substituted for stainless steel as the cladding material. Figures 2.21 and 2.22 are typical of such plates and show that good bonding may be obtained with matrices of iron or stainless steel without excessive diffusion.

With the hot-rolling technique a protective capsule or can is used to prevent oxidation of the clad compact during fabrication. Unless preventive steps are taken, the capsule bonds to the cladding plate, making separation impossible. Efforts are being made to prevent this bonding by applying a coating of Al_2O_3 to one of the surfaces. The most satisfactory separation was obtained when the Al_2O_3 was applied to the inner surface of the can by dipping it into a slurry of Al_2O_3 in clear lacquer. After air drying, the capsules were heated to 600°C in an oxidizing atmosphere to burn off volatile substances and residual carbon from the lacquer. With this technique separation of the can and compact was obtained after as much as 75% reduction. A few samples were not given the high-temperature treatment, with the result that, on heating for rolling, gas evolution caused a blistering of the capsule and contamination of all internal stainless steel surfaces.

Cladding Beryllium Oxide. It was desired to determine experimentally the feasibility of applying thin, adherent metal coatings to massive beryllium oxide blocks. A continuous metal envelope of the proper characteristics should afford increased thermal stress and shock resistance to the beryllia base. Also, any minor fracture or spalling of the refractory base would be confined.

[redacted]

Y-3939

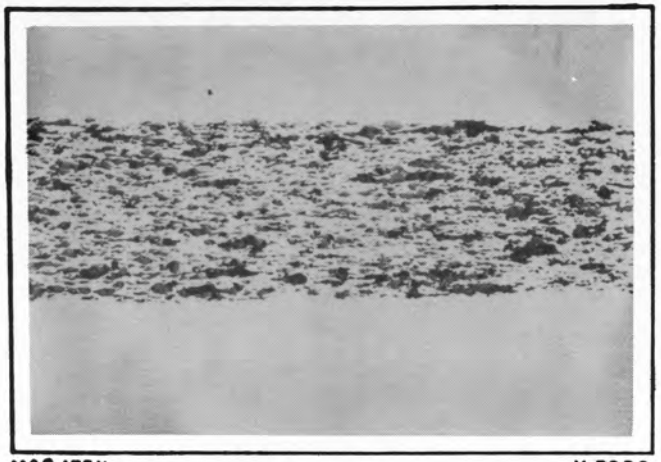

MAG. 175X Y-3229

-100 MESH

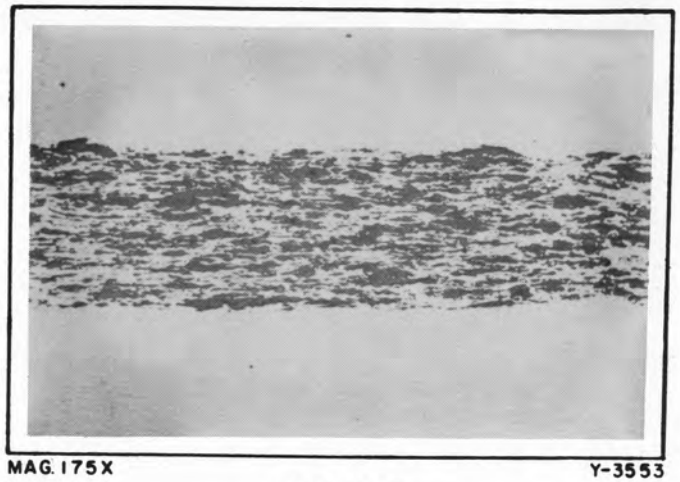

MAG. 175X Y-3553

-200 MESH

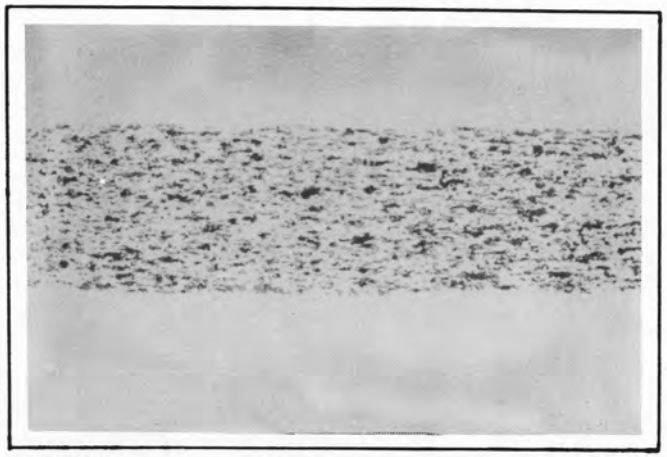

MAG. 175X Y-3550

-325 MESH

EFFECT OF STAINLESS STEEL PARTICLE SIZE ON UO_2 DISTRIBUTION

FIG. 2.19

[redacted]
Y-3937

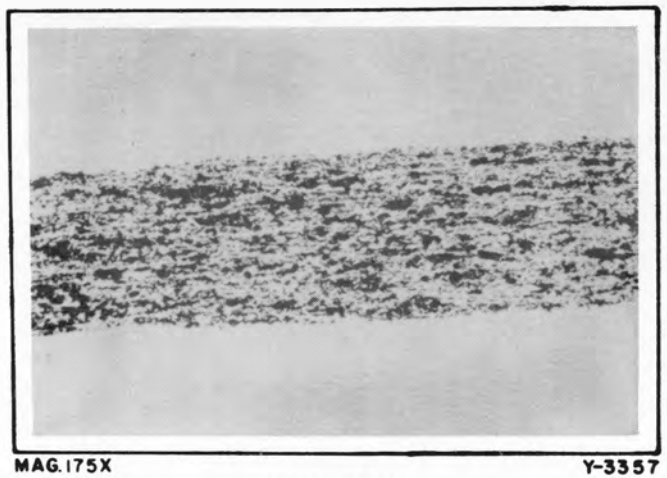

MAG. 175X Y-3357

-100 MESH

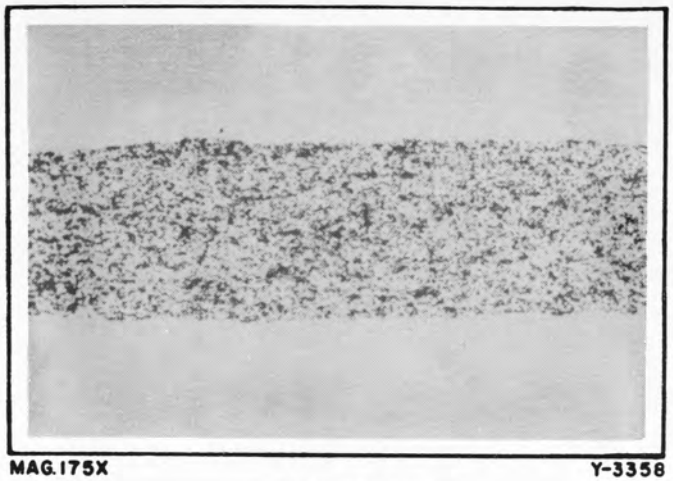

MAG. 175X Y-3358

-325 MESH

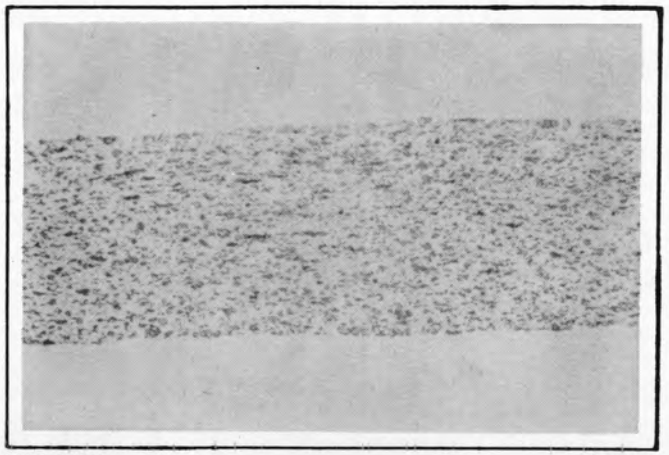

MAG 175X Y-3822

10 MICRONS

EFFECT OF IRON PARTICLE SIZE ON UO_2 DISTRIBUTION

FIG. 2.20

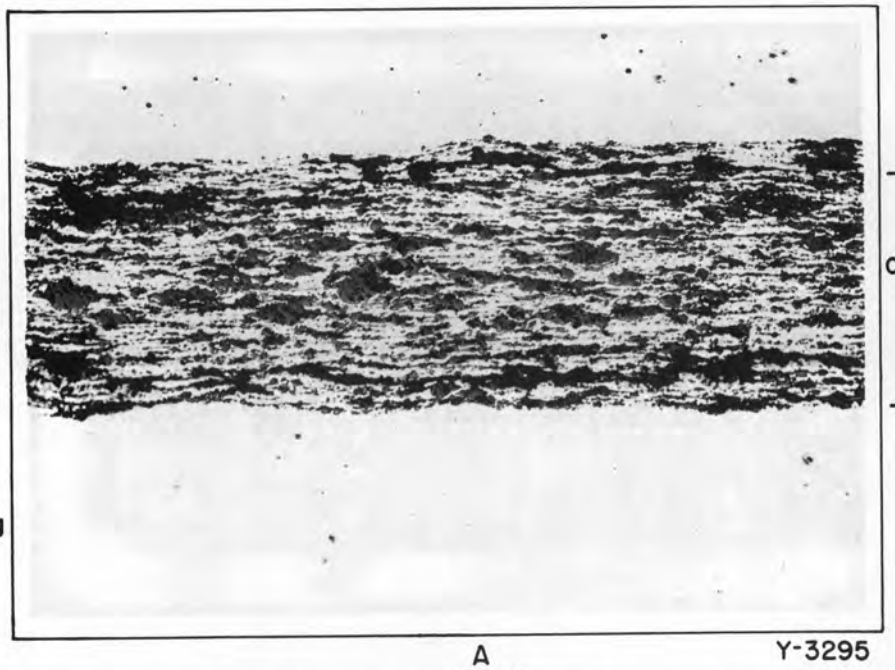

A
175 X
Y-3295

Double Inconel Clad Pressed 302-UO_2(50%) Compact, Hot Rolled 88%.

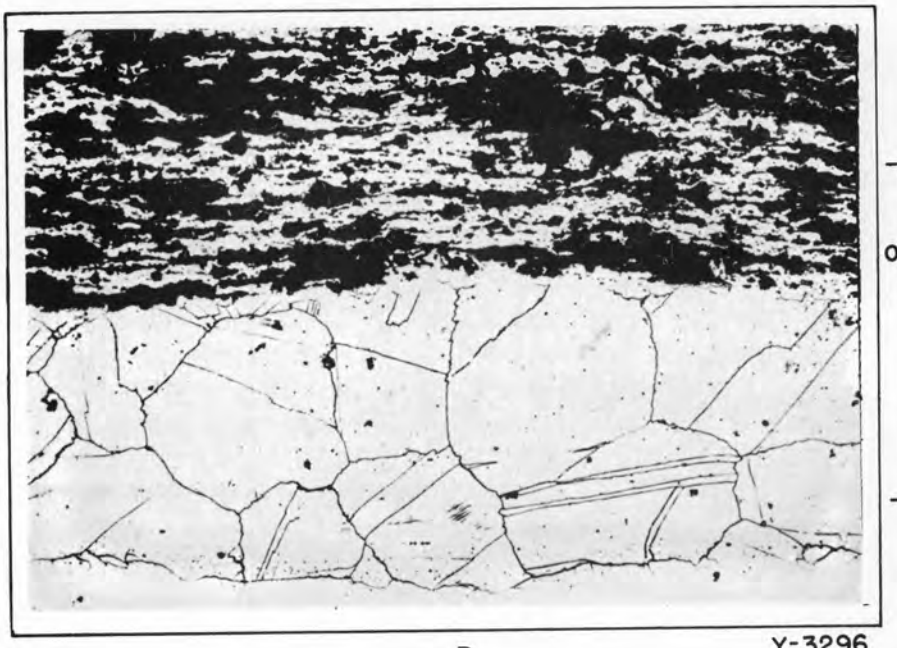

B
250 X
Y-3296

Above Specimen Etched In Aqua Regia.

FIGURE 2.21 DOUBLE CLAD, PRESSED, HOT ROLLED, 302 S.S.-UO_2 COMPACT-ETCHED & UNETCHED

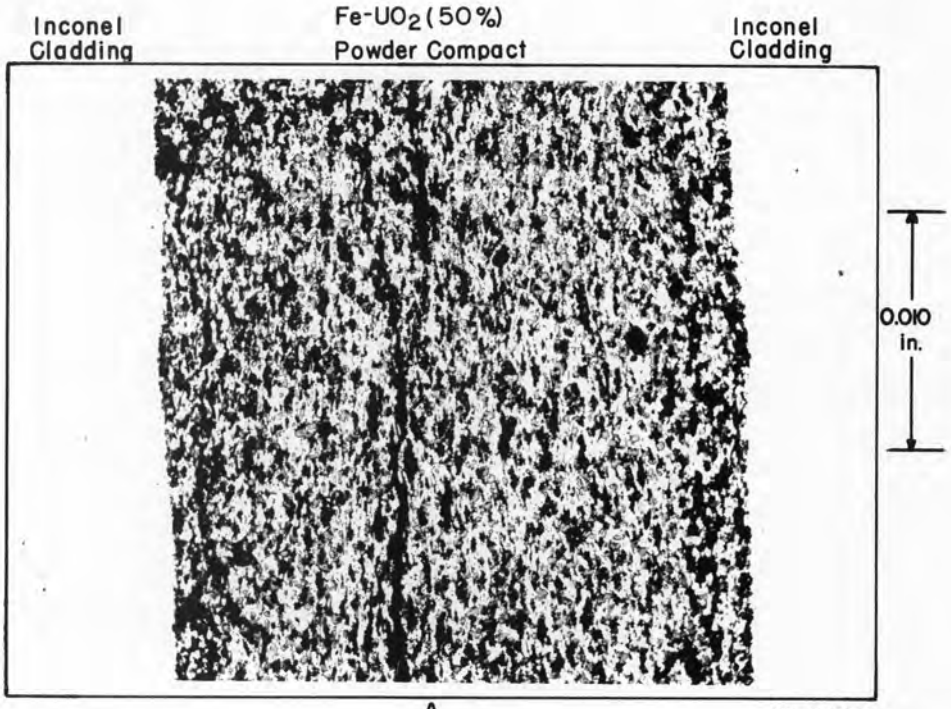

A
175 X
Y-3259
Double Inconel Clad Pressed Fe-UO_2(50%) Compact Hot Rolled 71%

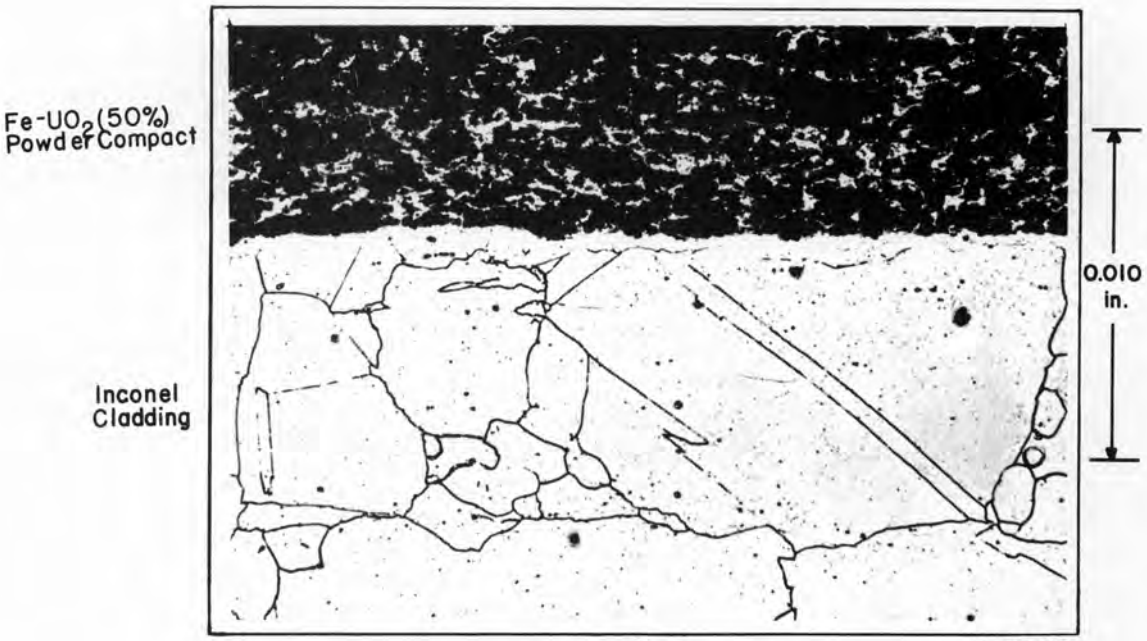

B
250 X
Y-3290
Above Specimen Etched In Aqua Regia.

FIGURE 2.22 DOUBLE CLAD, PRESSED, HOT ROLLED Fe-UO_2 COMPACT-ETCHED & UNETCHED

As a chemical type bonding of metal to nonporous ceramic (BeO) appears fundamental to the success of a coating, attempts were made to eliminate factors affecting mechanical adherence. Diamond-sawn surfaces of hot-pressed BeO (approximately 96% density) were used for test specimens. A Metallizing Engineering Company wire gun, Model 2E, was employed using either No. 18 or No. 20 B and S gauge wire. Spraying of the flat BeO surface measuring 3/4 by 1 in. was accomplished by several rapid passes, an air atmosphere being present in all tests. Reference to Table 2.6 indicates the conditions and qualitative degree of adherence observed.

The degree of adhesion is difficult to evaluate. however, it was found useful to deposit heavy coats (approximately 0.015 in. thick) of materials that apparently adhered strongly; and, in the case of nickel and types 304 and 410 stainless steel, the difference in thermal contraction on cooling to room temperature was sufficient to cause rupture of the massive BeO itself. With these three metals the mechanical stresses developed sheared off a shallow (about 1/16 in.) layer from the refractory. This same type of rupture occurred with 304 stainless steel sprayed on AlSiMag 491 preheated to 600°C. Grade 491 is a high-strength vitrified alumina body manufactured by the American Lava Corporation.

Metallographic examination of the interfacial zone between sprayed metal and ceramic is currently in progress (Fig. 2.23). Attempts are being made to evaluate the nature of the bond. In addition, several specimens of dense BeO will be metallographically polished prior to being metal sprayed. Under these refined surface conditions, analysis of the bond mechanism may be facilitated. Various high-temperature corrosion-resistant alloys with thermal expansions more similar to BeO are being considered. Materials such as hastelloy B, CM469, CM449, and stainless steel 446 and 430 are being obtained in wire or rod form.

Compatibility Tests of Potential Fuel Element Materials. Additional results of tests to obtain information on compatibility of possible high-temperature reactor constituents are reported in Table 2.7.

The test procedures and objectives are the same as outlined in the two previous Metallurgy Division quarterly progress reports (ORNL-987 and 910). Unless noted otherwise the samples were held at 1000°C for 100 hr.

NOT CLASSIFIED
Y-3950

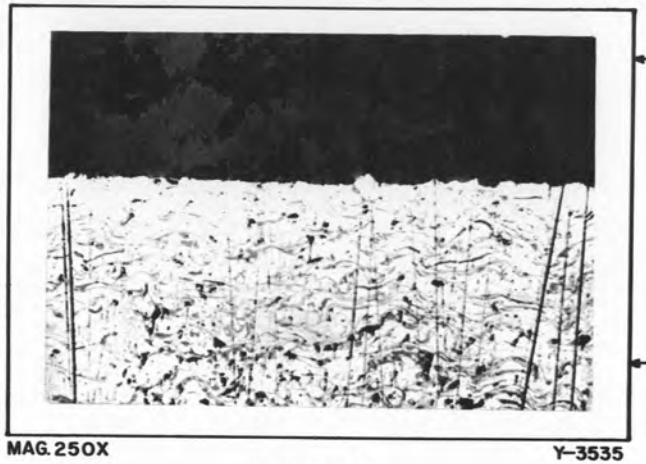

MAG. 250X Y-3535

SERIES "I"

BeO

Al_2O_3

304

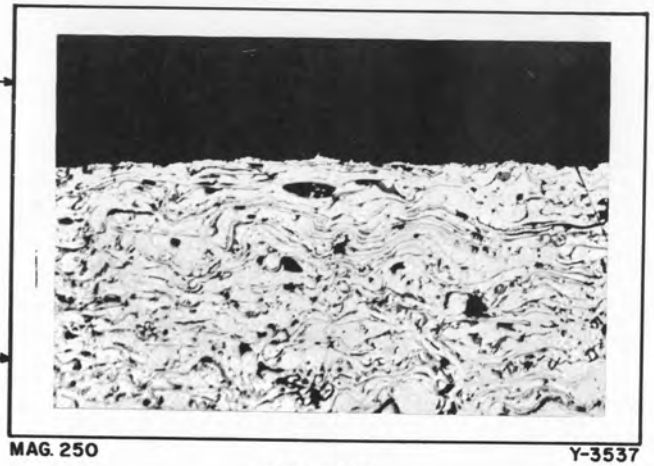

MAG. 250 Y-3537

SERIES "I"

UNETCHED

MAG. 250X Y-3533

SERIES "H"

BeO

410

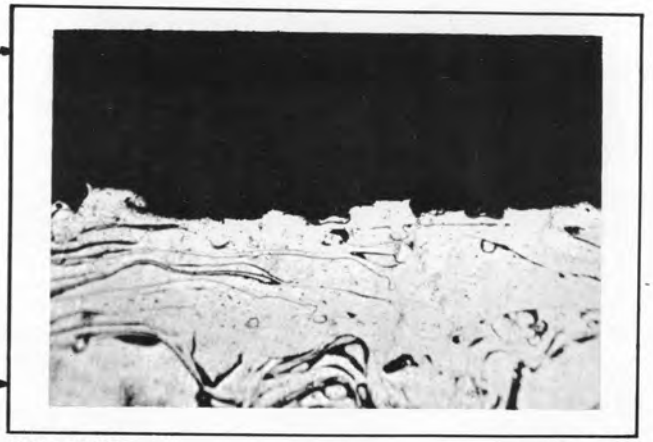

MAG. 1000X Y-3534

SERIES "H"

SPRAYED METAL INTERFACES

FIG. 2.23

TABLE 2.6

Metal Spray Coating of Ceramic Base

SERIES	METAL[a]	CERAMIC BASE	BASE TEMPERATURE OF PREHEATING (°C)	ADHERENCE	APPROXIMATE COAT THICKNESS (in.)	REMARKS
A	Monel	BeO, dense[b]	25	None	0.007	Loose sheet
			800	Slight	0.009	Discolored, knife-stripped easily, fairly brittle
B	Gold	BeO, porous[c]	25	Appears good		Clean
		BeO, dense	25	None	0.008	Loose sheet, ductile
		BeO, dense	600	Slight	0.006	Clean, knife-stripped easily, ductile
		BeO, dense	850	Slight	0.006	Clean, knife-stripped easily, ductile
		Al_2O_3, dense[d]	25	None	0.005	Loose sheet, ductile
C	Platinum	BeO, dense	25	None	0.008	Loose sheet, ductile
		BeO, dense	800	Slight	0.010	Knife-stripped easily, clean, ductile, some BeO adheres strongly to the platinum
D	Tantalum	BeO, dense	25	None	0.005	Slightly discolored, loose sheet, brittle
			600	Slight	0.011	Badly discolored, hard, brittle
E	Molybdenum	BeO, porous	25	Appears good		Clean
		BeO, dense	25	None	0.008	Clean, loose sheet, fairly brittle
		BeO, dense	600	None	0.014	Surface oxidation, brittle, knife-stripped easily
F	Aluminum	BeO, porous	25	Appears good		Clean
		BeO, dense	25	None	0.004	Clean, loose sheet, slightly ductile
		BeO, dense	600	Excellent	0.003	Clean, cannot be knife-stripped at interface[e]
G	Nickel	BeO, dense	25	None	0.006	Clean, loose sheet, fairly brittle
		BeO, dense	400	None	0.015	Clean, loose sheet, fairly brittle
		BeO, dense	600	None	0.025	Interface oxidized, loose sheet, fairly brittle
		BeO, dense	600[f]	Excellent	0.015	Clean; on cooling the BeO surface was completely sheared off
		BeO, dense	800[g]	Excellent	0.025	On cooling the BeO surface was completely sheared off

TABLE 2.6 (Cont'd)

SERIES	METAL[a]	CERAMIC BASE	BASE TEMPERATURE OF PREHEATING (°C)	ADHERENCE	APPROXIMATE COAT THICKNESS (in.)	REMARKS
H	410 stainless steel	BeO, dense	25	None	0.007	Clean, loose sheet, very slightly ductile
		BeO, dense	600	Excellent	0.025	Clean, BeO surface sheared off
I	304 stainless steel[h]	BeO, dense	25	None	0.008	Clean, loose sheet, very slightly ductile
		BeO, dense	600	Excellent	0.015	Clean, BeO surface sheared off
		Al_2O_3, dense	600	Excellent	0.017	Clean, Al_2O_3 surface sheared off

(a) Metallizing Engineering Company's wire gun No. 2E used, B and S, either No. 18 (approximately 0.040 in.) or No. 20 (approximately 0.032 in.).

(b) Dense BeO, $\rho = 2.87$ g/cc (approximately 5% porosity), hot pressed at 1850°C. Fine diamond-sawn to specimens approximately 1½ by 7/8 by 5/16 in. The entire 1½- by 7/8-in. face was coated.

(c) Porous BeO, $\rho \approx 2.1$ g/cc (30% porosity), slip-cast crucible by Brush Beryllium Company.

(d) Dense alumina, vitrified, about 5% porous. American Lava Corporation grade 491.

(e) During initial pass, sprayed-on aluminum had molten surface.

(f) BeO surface at 600°C first sprayed with one light pass of aluminum, then reheated to 600°C and a heavy nickel coat applied.

(g) No aluminum was used.

(h) All type 304 stainless steel sprayed deposits were weakly attracted by a magnet.

TABLE 2.7

Compatibility of Possible High-Temperature Reactor Constituents

MATERIALS	TEMPERATURE (°C)	REACTION LAYER (in.)	GAP (in.)	TOTAL (in.)
Beryllium-molybdenum	1000	0.011	0.003	0.014
Beryllium—430 stainless steel	1000	0.022	0.015	0.037
Beryllium-BeO	800 (195 hr)	No reaction		
Beryllium-BeO	1100	Very slight reaction if any		
Chromium-molybdenum	1000	0.001	0.005	0.006
Chromium-nickel	1000	0.003	0.001	0.004
Chromium-inconel	1000	0.006	0.002	0.008
Chromium—316 stainless steel	1000	0.003		0.003
Chromium-UO_2	1000	No reaction		
Chromium-BeO	1000	No reaction		
Iron—316 stainless steel	As swaged at 1000°C*	Slight diffusion zone		
Iron—316 stainless steel	800	0.001		0.001
Iron—316 stainless steel	900	0.011		0.011
Iron—316 stainless steel	1000	0.009	0.001	0.010
Iron—430 stainless steel	1000	0.002	0.011	0.013
Iron-UO_2	As sintered 14 hr at 1200°C*	No reaction		
Iron-UO_2	1000	No reaction		
Molybdenum-inconel	As swaged at 1000°C*	No reaction		
Molybdenum-inconel	800	0.003		0.003
Molybdenum—316 stainless steel	As swaged at 1000°C*	No reaction		
Molybdenum—316 stainless steel	1000	Trace	0.002	0.002
Nickel-BeO	1000	No reaction		
Inconel—304 stainless steel	1000	0.004		0.004
Inconel—316 stainless steel	900	0.004		0.004
Inconel-Be_2C	1000	0.003		0.003
Inconel-BeO	800	0.006		**
Tantalum—316 stainless steel	1000	0.014	0.001	0.015
302 stainless steel—316 stainless steel	900	Very slight reaction		
302 stainless steel—UO_2	As sintered 14 hr at 1200°C*	No reaction		
302 stainless steel—UO_2	1000	No reaction		
304 stainless steel—316 stainless steel	1000	No reaction		

*0 hr at temperature

**Presence of gap not determined. BeO powder fell out of capsule during cutting of sample

MECHANICAL TESTING

All 14 of the test chambers for the creep and stress-rupture testing programs have been received and assembled. Each chamber has been vacuum-leak tested with a helium leak detector, and all detectable leaks have been sealed. The vacuum systems operate in the pressure range of 0.01 to 0.05 μ Hg at 1000°C. The temperatures are controlled from the specimen surface, and the Leeds and Northrup D.A.T. control system maintains the temperature within ±1°C for an indefinite period of operation and for all temperatures from 70 to 1000°C.

Thermocouple instability has been suspected in these high-vacuum systems. The calibration of the couples can change owing to vaporization of alloying elements or to absorption of metal vapor from the specimen or from the chamber wall. To define the top temperature for high-vacuum operation in these metallic systems two experiments are being conducted. Three couples (platinum-platinum-10% rhodium, iron-constantan, and chromel-alumel) were placed in one of the test chambers and have been operating for 100 hr at 750°C and 0.04 to 0.05 μ Hg pressure. The chromel-alumel and the iron-constantan couples have remained constant as checked against a protected chromel-alumel couple, while the platinum couple has drifted 1°C in the same period. Following an additional 100 hr of operation this test will be repeated at successively higher temperatures, and the stability of each type of couple will be observed. Also, clean quartz tubes have been placed in several chambers and operated at different temperatures; no metal deposits have been observed at temperatures below 800°C, although at 850°C and above very extensive deposition occurs. In further study of thermocouple stability all couples will be calibrated before and after each test.

Uranium and thorium (0.505-in.) bar specimens and inconel and stainless steel sheet specimens are being machined. Sheet specimens are being cut with a "ball end" mill cutter. Experiments are being conducted to determine the feasibility of making the bar specimens in a milling machine with a formed flying cutter.

All machines have to be calibrated. These calibrations must include lever arm ratio, bellows spring rate, weights of pull rods, and pressure effects on the effective bellows area.

The 25-kw gasoline-powered emergency generator and transfer panel have been received and installed. This unit is automatic and will deliver full voltage within 30 to 60 sec after a power failure.

The horizontal temperature gradient in the test zone of the furnaces and the influence of the vertical gradient on the horizontal gradient are being investigated.

A preliminary program investigating elastic behavior at elevated temperature is being continued. About thirty tensile tests of various materials have been conducted as service to other sections.

WELDING LABORATORY

Welding of Inconel. A modified room-temperature tensile test has been used in the partial evaluation of weld quality of inconel tube-to-header welded joints. Test specimens were welded in pairs and pulled to destruction in a tensile jig as illustrated in Fig. 2.24.

Experiments to date have been confined to manual inert-arc welds. In view of the number of tube-to-header welds required for the ARE, the main portion of future work will involve use of semiautomatic "cone arc" apparatus,[1] the installation of which should be accomplished in the near future.

The effect of joint design on the room-temperature strength of manual inert-arc-welded joints has received some attention. Results of tests on inconel pairs incorporating complete penetration have exhibited strengths of 90,000 psi based on the tube dimensions of 0.187 in. O.D. and 0.030 in. wall. The overall pair length increased from 3 to 3.5 in., indicating approximately 16% average elongation.

Figure 2.25 is a typical inconel joint incorporating complete penetration. In view of the geometry of this type of joint, a failure in the heat-affected zone of the tubing would be expected.

(1) E. R. Mann, *Means for Making Uniform Circular Heliarc Welds by Deflecting the Ion Beam Continuously*, ANP-63 (April 9, 1951).

DWG. 11750
NOT CLASSIFIED

TENSILE TEST JIG FOR
TUBE-TO-HEADER WELDED JOINTS

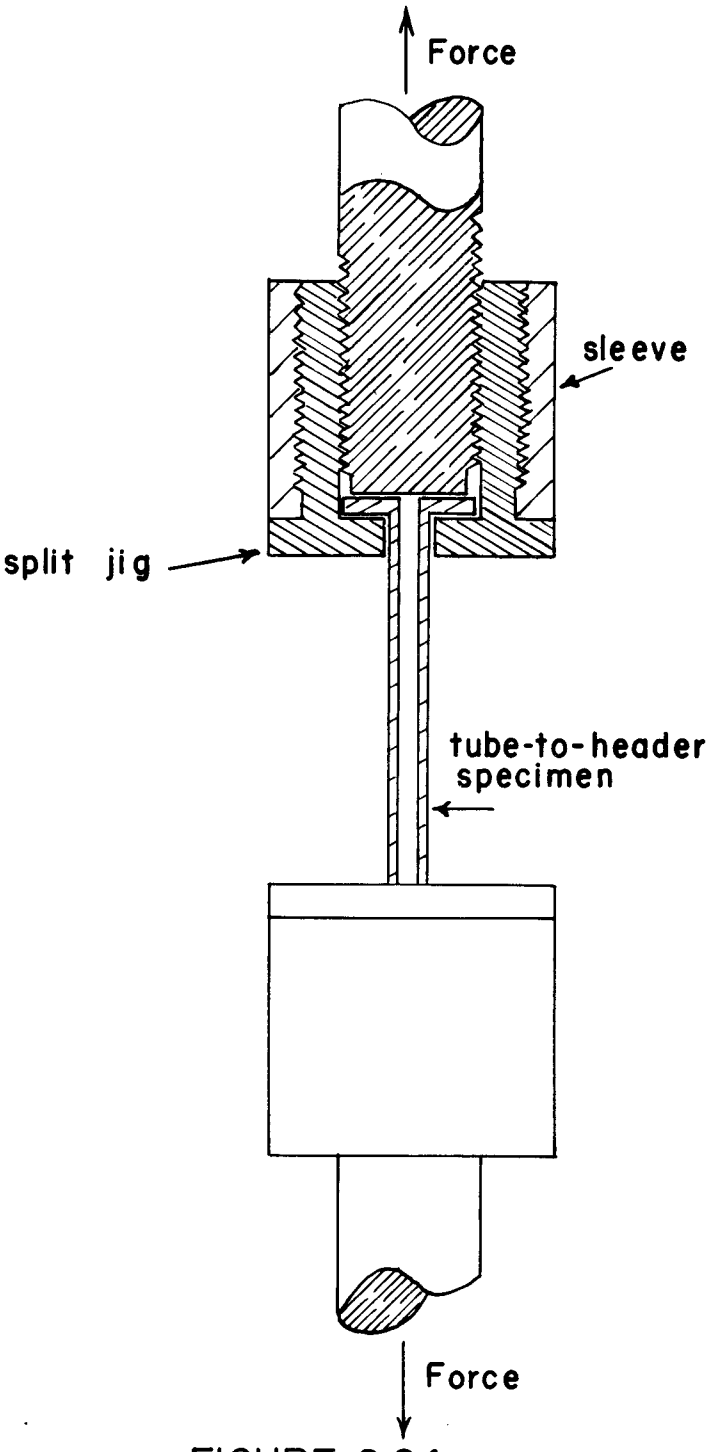

FIGURE 2.24

NOT CLASSIFIED
Y-3961

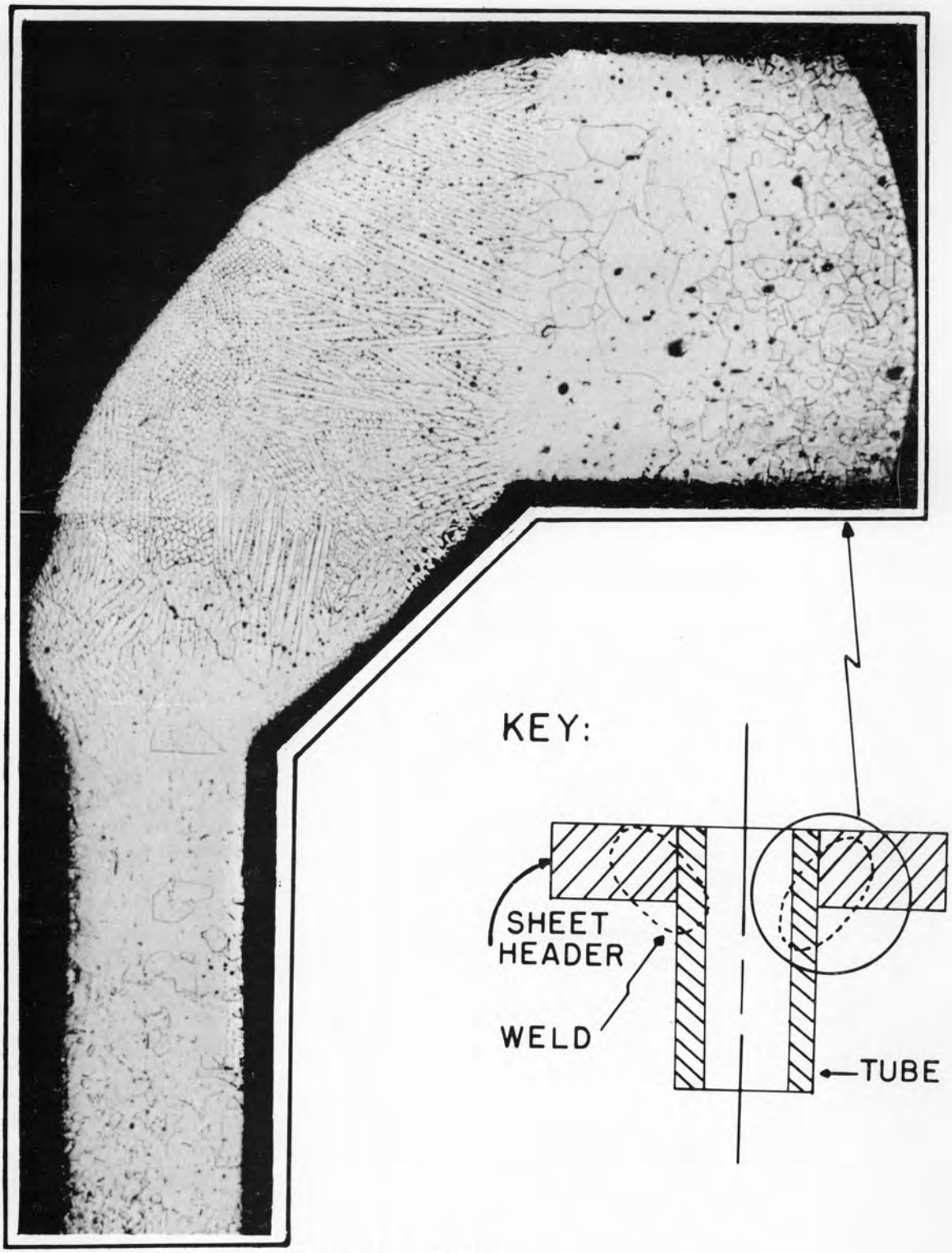

MAG. 50X Y-3946-Y-3948

CROSS SECTION OF INCONEL TUBE-TO-HEADER MANUAL INERT ARC WELD ETCHED WITH AQUA REGIA.

FIG. 2.25

Results on similar weld tests on pairs exhibiting incomplete penetration have been inconsistent. Strengths based on the tube dimensions varied from 57,000 to 84,000 psi. This may be attributed in part to difficulty of control of the degree of penetration during manual welding. Tests are contemplated on welded joints of this type which will be made using the cone-arc technique. It is expected that a given penetration can be consistently duplicated by proper control of the variables. A typical inconel tube-to-header weld made using the cone-arc technique and illustrating the type of joint incorporating incomplete penetration is shown in Fig. 2.26.

Corrosion tests, pressure tests, and fatigue tests will be included in future work, in addition to all weld-metal tests for basic evaluation of weld quality.

Welding of Refractory Elements. A subcontract is being arranged with Rensselaer Polytechnic Institute for the investigation of fusion and electric resistance welding of molybdenum.

Butt welds between 0.020 in. Fansteel columbium sheet have been made using the inert-arc process. Bend and transverse tensile tests indicate that welds in this material are relatively strong and ductile. Further work is contemplated.

PHYSICAL CHEMISTRY OF LIQUID METALS

The purpose of these studies is to determine what effect the orientation of a metal surface might have on the interaction between liquid and solid metals. The reasons for this investigation and the general method of study have been described previously in ORNL-987 (*Metallurgy Division Quarterly Progress Report for Period Ending January 31, 1951*).

Studies have been made of the action at room temperature of small amounts of liquid mercury on copper single crystals. These studies show that the interaction of liquid mercury and solid copper varies considerably with crystal orientation.

The copper specimens were in the form of spherical single crystals 5/8 in. in diameter. The surfaces of these crystals were electrolytically polished until smooth and free from mechanical strain.

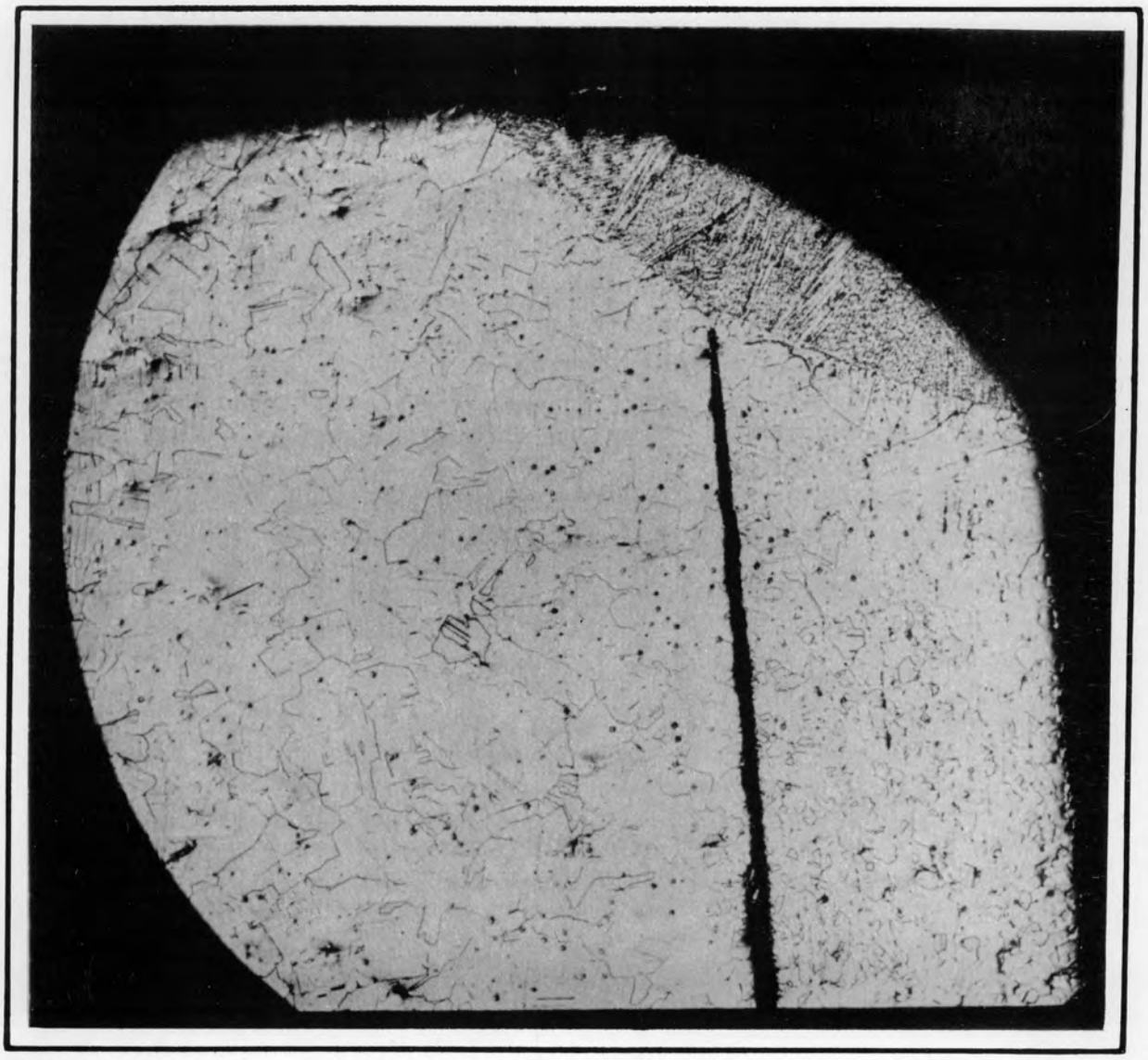

MAG. 50X ETCH: AQUA REGIA Y-3700

CROSS SECTION OF INCONEL TUBE-TO-HEADER INERT "CONE-ARC" WELD.

FIG.2.26

Interaction in the Presence of Air. Copper crystals were immersed in liquid mercury in the presence of air. After 1 hr they were removed, and it was found that certain crystallographic regions were uniformly covered with a film of mercury while the remaining regions were covered with small isolated mercury droplets. Figure 2.27 is an approximate stereographic plot of the appearance of the surface of the sphere. The plot is oriented so that a (100) pole occurs at the center of the circle. Four other (100) poles occur on the periphery of the plot as marked with arrows. The shaded regions were covered with fine droplets. The unshaded regions were covered with a uniform film, the boundary lines of which were very smooth and sharply defined. This experimental result could be reproduced only when care was taken to avoid contaminating the crystal surface with traces of grease or other foreign material before immersion in the mercury.

Interaction in the Presence of Hydrogen. Copper single crystal spheres were annealed in hydrogen at 550°C for 4 hr to remove oxide films. After cooling to room temperature the crystals were immersed in mercury without exposure to the air. On removal it was found that they were uniformly covered with a thin mercury film. Specimens covered with such a film were allowed to stand without being reimmersed in mercury, and after a week a pattern of smooth and rough areas had formed on the surface of the sphere. Figure 2.28 is an approximate stereographic projection of this pattern, which has the same orientation as Fig. 2.27. The unshaded areas denote the smooth regions. The shaded areas denote the roughened regions. The line separating smooth and rough regions was not sharply defined. Figure 2.29 is a photograph taken normal to a [100] axis of one specimen. Strong specular reflections were obtained from the (100) regions from a beam of light directed normal to a [100] axis and from a beam normal to a [111] axis. Microscopic examination showed that the roughness was produced by small crystallites. In the neighborhood of a (100) pole the crystallites had one face parallel to the (100) plane.

The importance of these experiments has been to show that in at least one situation the interaction of a liquid and a solid metal is influenced by crystal orientation.

DWG.11749
NOT CLASSIFIED

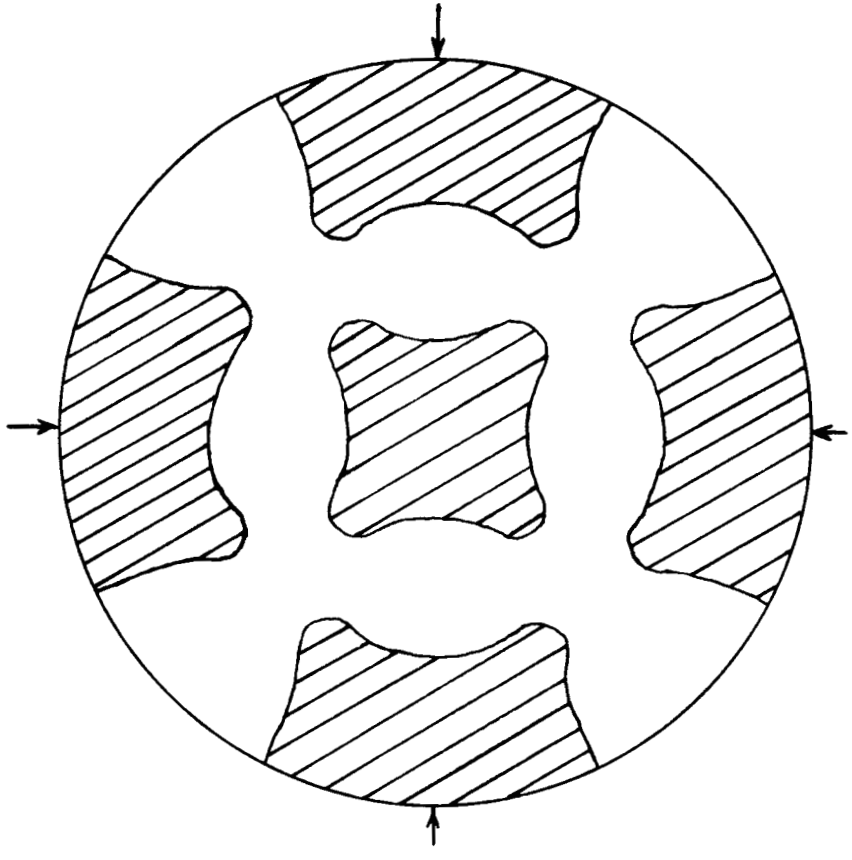

Stereographic projection of the action of liquid mercury on a copper single crystal sphere in air.

FIGURE 2.27

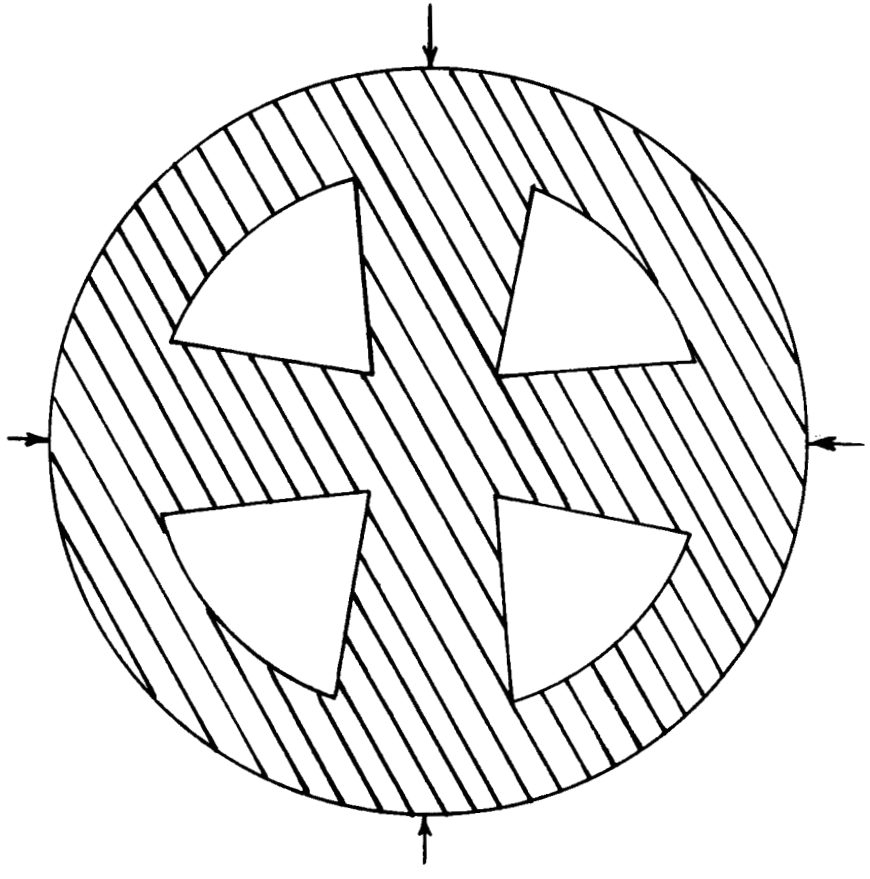

Stereographic projection of the action of liquid mercury on a copper single crystal sphere in hydrogen.

FIGURE 2.28

G.P. Smith

UNCLASSIFIED

Y-4081

Y-3998 4X

ACTION OF MERCURY ON A SINGLE CRYSTAL SPHERE IN AN ATMOSPHERE OF HYDROGEN.

FIG. 2.29

3. MTR FUEL UNITS

The starting date for fabrication of the MTR fuel units for the Idaho site has been changed from March 1, 1951 to July 1, 1951 to minimize holdup of enriched U^{235}. On the basis of an MTR start-up date of October 1, 1951, the new schedule requires that two reactor loadings, or 46 fuel assemblies and eight shim rod elements, be available by mid-September and that the fabrication of an additional 84 fuel elements be completed by January 1, 1952.

At present 25 natural-uranium fuel units are being prepared for the Chemical Technology Division for use in their dissolving tests on the RaLa program. Fabrication work on these units is estimated to be about 20% complete.

4. X-RAY LABORATORY

EFFECT OF PRECIPITATION IN COPPER-BERYLLIUM ALLOYS

A study of the nature of the precipitation process in copper-beryllium has been undertaken. Spectrometer traces of alloys aged for various temperatures and times have been made in an effort to find a range of values for these two variables which would permit the most effective study of the effect of precipitation. New, carefully homogenized samples are currently being prepared for quantitative measurements.

HOT-LABORATORY SPECTROMETER DESIGN

The design of an X-ray spectrometer for radioactive samples has been completed and is now being built. A Hilger X-ray diffraction unit has been purchased and will be used as a power source for the spectrometer. It is expected that the initial tests of this instrument will take place late this summer.

ROOM-TEMPERATURE RECOVERY IN COPPER

Recovery in copper at room temperature is being investigated by X-ray methods. Unannealed filings, cut from a solid specimen, were passed through a 100-mesh screen and pressed with a spatula into a small plastic sample holder. A small amount of grease was used as an adhesive. The powder pattern of the sample was then observed with a high-angle North American Phillips X-ray spectrometer. Figure 4.1 shows a comparison of the (331) line of the copper pattern at various times after the sample was prepared. After about one month no difference between the filings and an annealed specimen could be detected.

An analysis of the distortions normal to the (331) planes was made, using the method of Warren and Averbach.[1] The approximation

(1) B. E. Warren and B. L. Averbach, "The Effect of Cold-Work Distortion on X-Ray Patterns," *J. Applied Phys.* 21, 595 (1950).

DWG.11748
NOT CLASSIFIED

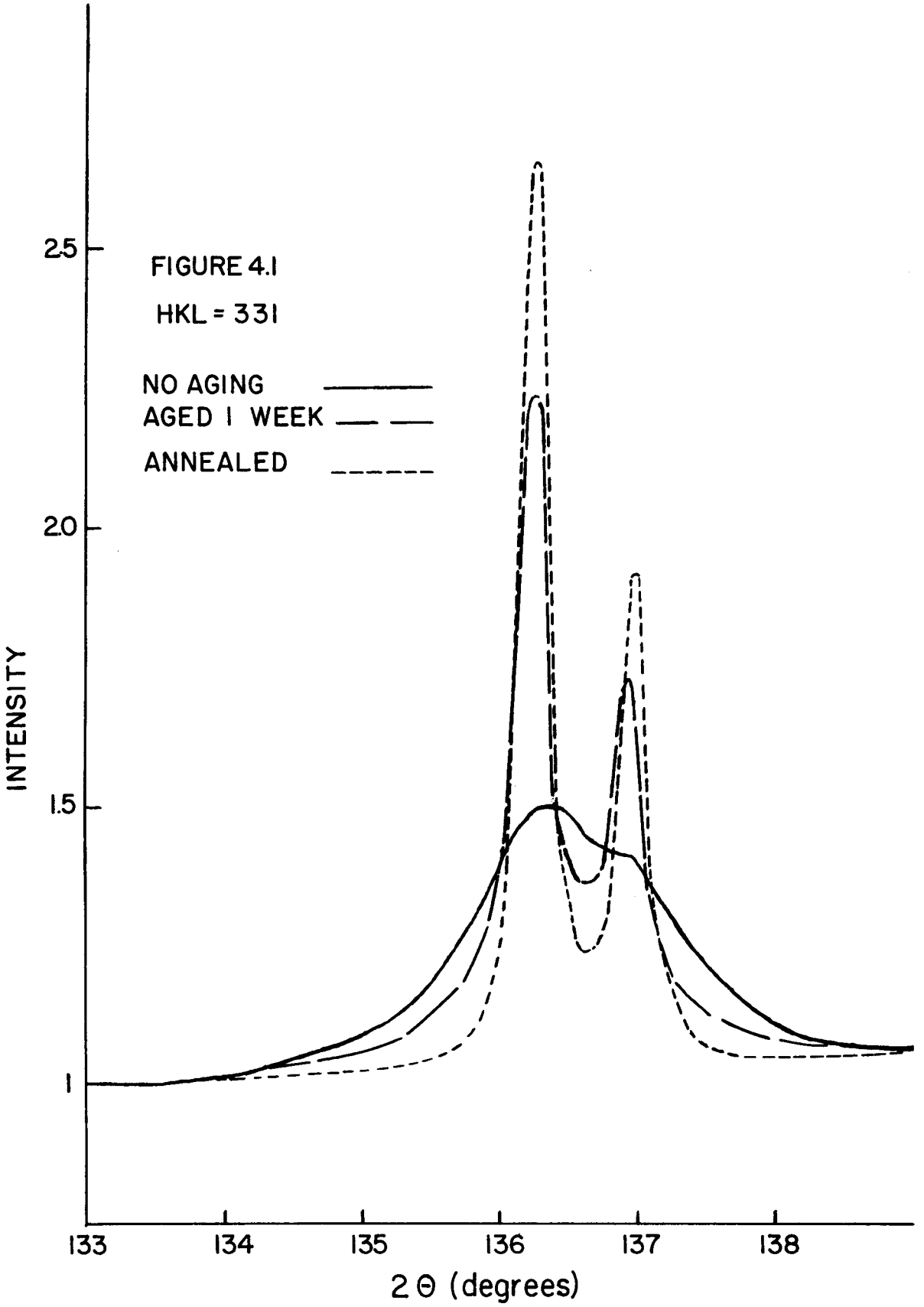

$$\cos 2\pi \frac{\Delta L}{d} \approx \exp \left[- \frac{2\pi^2}{d^2} (\Delta L^2) \right]$$

was used, and all instrumental contributions to the line contour were eliminated by the method of Stokes.[2] The results of this analysis are shown in Fig. 4.2. The quantity ΔL, plotted on the ordinate, is the root mean square change, upon cold working, in the length of a column of diffracting material originally L units long. The length L is chosen so that it is normal to the reflecting planes.

Certain features of the curves of Fig. 4.2 are of significance. Except for the $t = 0$ curve (plotted from data taken the day the material was cold worked), all of them saturate, and the position of the knee is in approximately the same place ($L = 20$ to 30 Å). The main difference in the curves, except $t = 0$, is that the level of the plateau decreases with time.

These characteristics of the data may be explained in the following way: Suppose that the density of the regions of distortion — or dislocations — is high immediately after cold working. Then ΔL should continue to change with L since a column of diffracting material is composed mostly of distorted regions.

Now suppose that, some time later, the density of dislocations has become considerably less, so that the probability of a column of length L passing through more than one dislocation is small. Then if R is the dimension of a distorted region normal to the reflecting planes, as long as L is less than R, ΔL should continue to change with L. But for L greater than R, ΔL should become constant since at least a length $L - R$ of the column must extend into the undistorted portion of the sample.

The fact that the knee in the curves of Fig. 4.2 does not move with time implies that the size of a distorted region remains unchanged. If the number of such regions remained constant but each region slowly decayed, then the knee should move toward the origin. Hence the distorted regions are, in a

(2) A. R. Stokes, "A Numerical Fourier-analysis Method for the Correction of Widths and Shapes of Lines on X-Ray Powder Photographs," *Proc. Phys. Soc.* 61, 382 (1948)

DWG. 11747
NOT CLASSIFIED

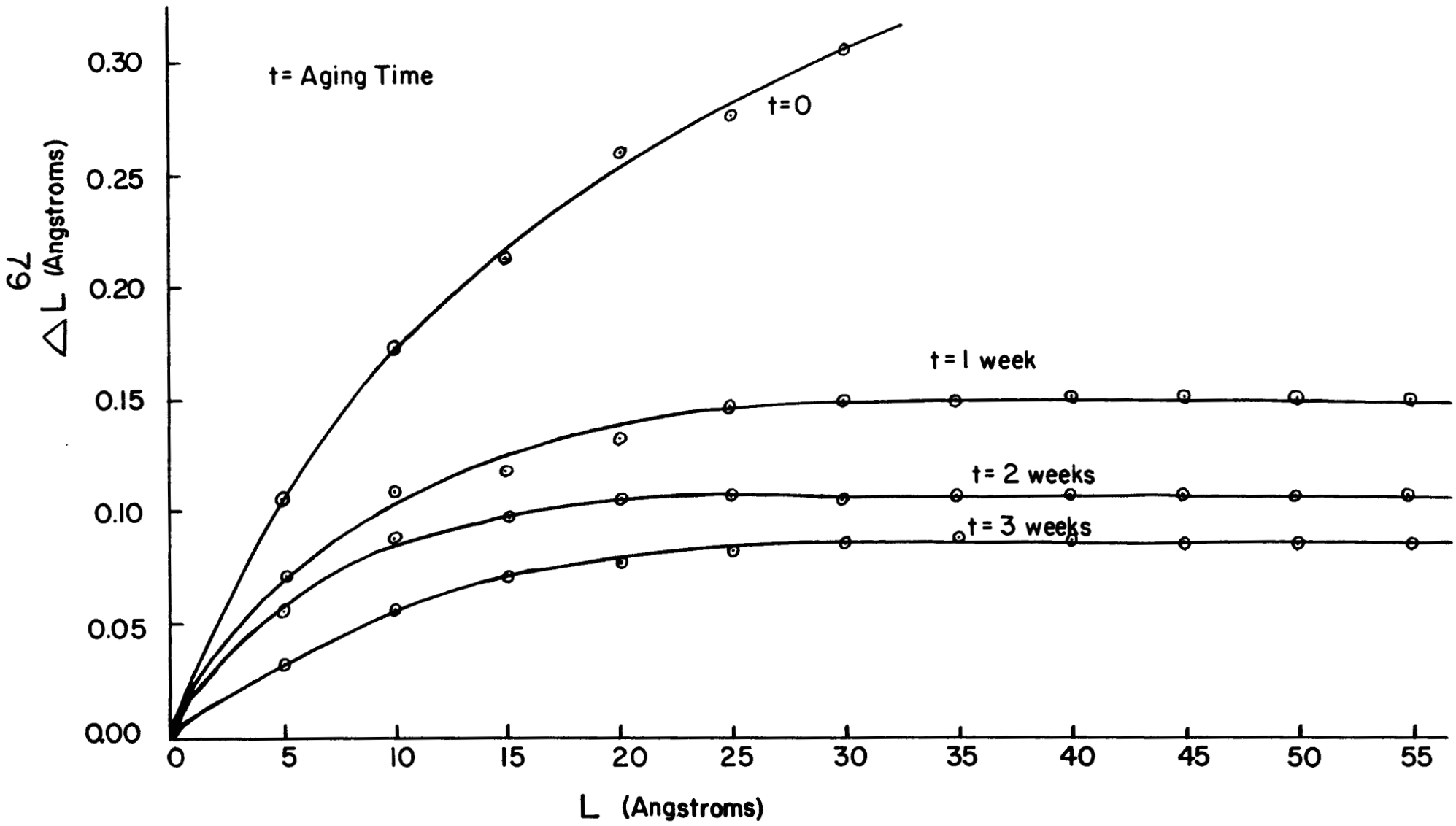

sense, quantized. Unless a distortion is annihilated (by diffusion to the grain boundary, for instance) it remains in its original form. The lowering of the plateau with time may be explained by the fact that as the density of distortions becomes less, the probability of a column of length L passing entirely through undistorted material becomes greater. Such columns, of course, make no contribution to the root mean square average of ΔL.

These findings appear to be entirely consistent with the dislocation theory. The position of the knee, about 10 atom diameters from the origin, is in agreement with that predicted by the theory.

Further investigations of this type of other crystallographic planes of copper are in progress.

5. SERVICE WORK

ROLLING MILL SECTION

ANP Disks. A total of 4176 enriched U^{235} (process level) metal disks were fabricated for use in conducting the ARE criticality experiments at the Y-12 site. Specifications on each of the four disk sizes required and the number of each prepared are:

QUANTITY	OUTSIDE DIAMETER (in.)	INSIDE DIAMETER (in.)	THICKNESS (in.)	MASS (g)
2066	2.858 ± 0.002	0.196 ± 0.002	0.0090 0.0095	17.1 to 18.1
2076	1.429 ± 0.001	0.196 ± 0.002	0.0090 0.0095	4.42 to 4.52
16	2.858 ± 0.002	0.196 ± 0.002	0.0018 0.0022	3.6 ± 0.1
18	1.429 ± 0.001	0.196 ± 0.002	0.0018 0.0022	0.9 ± 0.1
4176				

U^{235} metal ingots weighing about 1 kg, and approximately 4 by 7 by 1/8 in. thick, were supplied by Y-12. Initially these ingots were cold-rolled to 0.050 in. thickness; they were then jacketed in a soft iron case and hot-rolled at 1200°F to within a few mils of desired thickness and were finally stripped of the iron jacket and cold-rolled to finished thickness.

Disks of appropriate sizes were punched from the thin uranium foil, using a punch and die set. All disks were pickled in cold concentrated HNO_3 to remove the thin oxide film and to adjust the weight downward to meet tolerance.

Boral Sheet. Several hundred feet of boral sheet were rolled for the Reactor Technology Division. Powdered graphite was used between the boral ingot and the aluminum jacket to prevent bonding.

Spacer Rod. Five hundred lineal feet of 347 stainless steel spacer rod of special cross-section was prepared for the ANP Heat Exchanger Group at Y-12.

KAPL Washers. The thin U^{235} washers and foil requested on orders SR-SNY-344 and SR-SNY-346 have been fabricated to specifications and forwarded.

X-RAY LABORATORY

During this period 295 X-ray diffraction patterns were measured as a service activity for other research groups. Fifty-nine percent of these patterns were for projects of the Metallurgy Division, 22% for the Physics of Solids Institute, 13% for the Chemistry Division, and 6% for the Physics Division.

Slightly more than half the patterns taken were for identification purposes. Satisfactory identification was accomplished for almost 90% of the samples examined. New compounds of unknown composition and structure probably account for most of the unidentified patterns.

In addition to identification problems, the service work of the laboratory during this period included single crystal orientation measurement, preferred orientation studies, and purity checks.

POWDER METALLURGY SECTION

Lengths of inconel tubing were surface decarburized for the Corrosion Group. This was done by passing wet hydrogen through them at 1000°C. Samples held 66 hr showed definite decarburization while after 13 hr it was questionable.

At the request of the Reactor Technology Division an attempt was made to fabricate a stainless steel bearing containing MoS_2. The Cincinnati Milling Machine Company has agreed to attempt to press such a bearing directly, so the attempt here was to impregnate a porous stainless steel sheet. Various pressed compacts of iron, iron oxide, and MoS_2 were placed on the porous sheet and held at 1000°C; however, no impregnation took place. Further tests will be made at higher temperatures and with more intimate contact of the iron-MoS_2 layer and the stainless steel sheet.

Several high-density randomly oriented aluminum slugs were fabricated and sintered at the request of the Fundamental Research Section.